Electronic Supplementary Material (ESI) for Organic Chemistry Frontiers.

Supporting Information

1. Experimental Details

Materials. Commercially available starting materials were used as received without further purification. Cucurbit[8]uril (CB8) was synthesized according to reported procedures.[1] All solutions were prepared in ultrapure water from Millipore water purification system unless otherwise stated. CB8 solutions were titrated with cobaltocenium following a reported protocol.[2] Solvents were dried before use with molecular sieves. Silica gel for chromatography (Carlo Erba 40-60 μm, 60 Å) was used for column chromatography and TLC was performed on MN ALUGRAM Xtra SIL G UV254 TLC plates employing 254 nm and/or 366 nm UV-lamp for visualization.

General Methods. UV/vis absorption spectra were recorded using a Varian Cary 100 Bio or a Varian Cary 5000 spectrophotometer in quartz or disposable plastic cuvettes with 10 mm optical path. NMR spectra were recorded on a 400 MHz (100 for ^{13}C) Bruker Avance III 400 or 500 MHz (125 MHz for ^{13}C) Bruker AVANCE Neo 500 spectrometer at 25 °C using standard pulse programs. Residual solvent signals were used for calibration (^{1}H: $\delta(CHCl_3)$ = 7.26 ppm, $\delta(CHD_2OD)$ = 3.31 ppm; ^{13}C: $\delta(CDCl_3)$ = 77.00 ppm, $\delta(CD_3OD)$ = 49.00 ppm). Low resolution mass spectrometry was performed on an Agilent 6130B Single Quadrupole LC/MS (with an ESI source and coupled to an HPLC Agilent 1200 series) apparatus. High resolution mass spectrometry was performed on a LTQ OrbitrapTM XL hybrid mass spectrometer (Thermo Fischer Scientific, Bremen, Germany) controlled by LTQ Tune Plus 2.5.5 and Xcalibur 2.1.0. Elemental analysis was performed on a Thermo Finnigan-CE Instruments Flash EA 1112 CHNS series apparatus.

Isothermal Titration Calorimetry (ITC). The experiments were performed on a Nano ITC (TA Instruments) with standard volumes. The solutions were thoroughly degassed before use by stirring under vacuum. The sample cell was loaded with the CB8 solution

and a 250 µl autopipette was filled with the guest solution. The host was titrated in a sequence of either 50 injections of 5 µl or 25 injections of 10 µl after reaching baseline stability. The heat of dilution was corrected by injecting the guest solution into ultrapure water and subtracting these data from those of the host-guest titration.

Photochemistry. Continuous irradiations experiments were conducted in a Spex Fluorolog-2 Model F111 spectrofluorometer equipped with a 150 W Xe lamp or in a custom photochemical reactor equipped with a 200 W Hg-Xe lamp and using bandpass or cut-off filters to isolate the desired wavelengths. The light flux (I_0) was determined using as actinometers, ferrioxalate in water for λ_{irr} = 365 nm and the diarylethene derivative 1,2-bis(2,4-dimethyl-5-phenyl-3-thienyl)perfluorocyclopentene in hexane for λ_{irr} = 550 nm.[3] Photochemical quantum yields (Φ) were determined from equation (1), where $\Delta A/\Delta t$ is the slope of the plot obtained by measuring the absorbance of the product or reactant against the irradiation time, V is the irradiated volume, ε is the molar extinction coefficient of the product or reactant (depending on which species is being monitored) and A_{irr} is the initial absorbance at the irradiation wavelength,

$$\emptyset = \frac{n\ moles\ of\ product\ per\ unit\ time}{n\ moles\ of\ absorbed\ photons\ per\ unit\ time} = \frac{\frac{\Delta A}{\Delta t \cdot \varepsilon} \cdot V}{I_0\left(1 - 10^{-A_{irr}}\right)} \qquad (1)$$

The isomeric content of the photostationary states (PSS), produced upon irradiation of the open DTE isomers with λ_{irr} = 365 nm, were straightforwardly determined by integration of the ^{1}H NMR signals, assigned to the open and closed DTE isomers, in the respective spectra acquired for the PSS. For DTE's **3** and **4**, which are not quantitatively converted into the respective closed isomers, aliquots of the solutions, with known

open:closed isomeric ratio, were taken from the NMR tubes and transferred into quartz cells. These aliquots were diluted with MQ water to obtain suitable concentrations for the acquisition of the respective UV-Vis absorption spectra. These spectra were then used together with the ones of the pure open forms, to compute the spectra of the closed isomers by spectral decomposition. With the spectra of the opens and closed isomers in hand, the composition of PSS produced upon irradiation with other wavelengths (i.e. λ_{irr} = 334 nm) can be determined by spectral decomposition.

2. Synthesis and Characterization

Compounds **1** – **4** were synthesised according to scheme S1 by following and/or adapting previously reported protocols.[4–7] Methylation of 3-methylthiophene **11** afforded 2,4-dimethylthiophene **13**. Chlorination of **13** with SO_2Cl_2 to yield **15** was followed by Friedel-Crafts acylation using glutaryl chloride. The obtained diketone **17** originated the dithienylethene **19** by means of a McMurry olefination using $TiCl_3(THF)_3$. Suzuki coupling with 4-bromopyridine yielded the bis(pyridinyl)dithienylethene **23**. The corresponding salt **1** was obtained upon reaction with MeI. Compounds **2**, **3** and **4** were synthesized by analogous procedures, starting from 2-methylthiophene **9**. Reaction of the corresponding dithienylethene **18** with 4-, 3- or 2-bromopyridine afforded **20**, **21** and **22**, that in turn gave **2**, **3** and **4,** respectively. Compounds **21**, **23**, **1**, **3** and **4** were synthesised for the first time. Spectroscopic data for the remaining compounds are in accordance with the literature references: compounds **13**, **15**, **17**, and **19** were previously reported by Gostl *et al.*;[4] compounds **14**, **16**, and **18** by Yu *et al.*;[6] compounds **20** and **2** by Yao *et al.*;[5] and compound **22** by Tan *et al.*.[7]

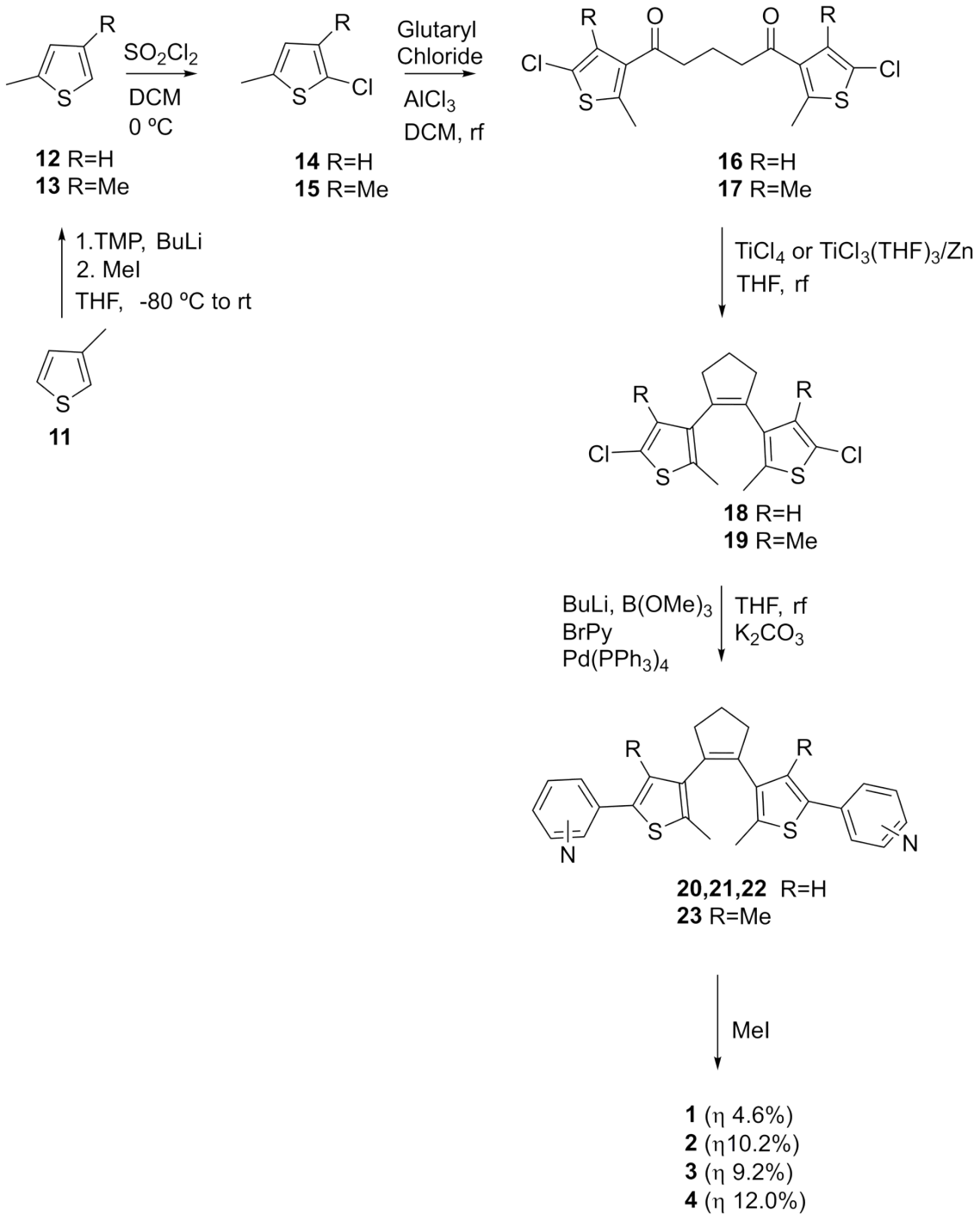

Scheme S1 – Adopted synthetic scheme for the synthesis of DTEs **1**, **2**, **3** and **4**.

*Synthesis of 2,4-dimethylthiophene (**13**)*

To 1 ml (0.837 g, 5.9 mmol) of 2,2,6,6-tetramethylpiperidine in 15 ml of dry THF, under nitrogen, at -80 ºC, 4.8 ml (7.7 mmol) of *n*-butyllithium solution (1.6 M) were slowly added. After 30 min., 500 µl (508 mg, 5.2 mmol) of 3-methylthiophene **11** were added. After another 30 min., 500 µl (1.14 g, 8.0 mmol) of iodomethane were added, and the reaction was now allowed to proceed at room temperature for 1 h 20 min. After this time HCl 1M was added and the crude was extracted with diethyl ether. The organic layer was washed with saturated $NaHCO_3$ solution, dried with Na_2SO_4, filtered and carefully evaporated to dryness, yielding 2,4-dimethylthiophene **13**. The product was used in the following reaction without further purification.

^{1}H NMR (400 MHz, $CDCl_3$) δ: 6.64 (*s*, 1H), 6.57 (*s*, 1H), 2.44 (*s*, 3H), 2.20 (*s*, 3H).

*Synthesis of 2-chloro-3,5-dimethylthiophene (**15**)*

To a solution of the previously prepared 2,4-dimethylthiophene **13** in 15 ml of dry dichloromethane, under nitrogen, in an ice-water bath, 450 µl (749.2 mg, 5.56 mmol) of SO_2Cl_2 were slowly added. After 20 min, total consumption of the starting material was observed and the reaction was cautiously quenched with water. The product was extracted with dichloromethane, dried with Na_2SO_4, filtered and cautiously evaporated to dryness, yielding 2-chloro-3,5-dimethylthiophene **15**. The product was used in the following reaction without further purification.

^{1}H NMR (400 MHz, $CDCl_3$) δ: 6.43 (*s*, 1H), 2.36 (*s*, 3H), 2.10 (*s*, 3H).

*Synthesis of 1,5-bis(5-chloro-2,4-dimethylthiophen-3-yl)pentane-1,5-dione (**17**)*

To 383.9 mg (2.62 mmol) of the previously prepared 2-chloro-3,5-dimethylthiophene **15** in 5 ml of dry dichloromethane, under nitrogen, in an ice-water bath, 200 µl (264.8 mg, 1.57 mmol) of glutaryl chloride were added, followed by the careful addition of 556.8 mg (4.19 mmol) of $AlCl_3$. The reaction was then allowed to proceed at reflux for 1h, time after which total consumption of the starting material was observed. The reaction was quenched by the careful addition of water at 0 ºC, and the crude was extracted with dichloromethane. The gathered organic phases were dried with Na_2SO_4, filtered and evaporated to dryness. Purification by flash chromatography using a mixture of *n*-hexane/EtOAc - 85/15 yielded 167.2 mg (0.58 mmol, 44.3%) of the diketone **14**.

^{1}H NMR (400 MHz, $CDCl_3$) δ: 2.82 (*t*, J=6.9, 4H), 2.48 (*s*, 6H), 2.20 (*s*, 6H), 2.11-2.04 (*m*, 2H).

*Synthesis of 1,2-bis(5-chloro-2,4-dimethylthiophen-3-yl)cyclopent-1-ene (**19**)*

In a double neck flask with 673 mg (1.82 mmol) of $TiCl_3(THF)_3$ degassed, under nitrogen, 5 ml of dry THF were added. After cooling in an ice-water bath, 247.5 mg (3.78 mmol) of Zn dust were added under nitrogen, and the mixture was refluxed for 45 min. After this time a solution of 97.4 mg (0.25 mmol) of the diketone **17** in 1ml of dry THF, was added at 0 ºC. The reaction was allowed to proceed at reflux for 1 h 45 min, time after which total consumption of the starting material was observed. After cooling at 0 ºC, the reaction was quenched with a 10% K_2CO_3 solution and filtered through a pad of celite. The filtrate was dried over Na_2SO_4, filtered, and evaporated to afford dithienylcyclopentene **19**. Purification by flash chromatography using *n*-hexane as eluent yielded 26.4 mg (0.074 mmol, 29.6%).

^{1}H NMR (400 MHz, $CDCl_3$) δ: 2.70 (*bs*, 4H), 2.08-1.96 (*bm*, 14H).

*Synthesis of 1,2-bis(2,4-dimethyl-5-(pyridin-4-yl)thiophen-3-yl)cyclopent-1-ene (**23**)*

To 80.9 mg (0.23 mmol) of the dithienylcyclopentene **19** in 5 ml of dry THF, degassed, under nitrogen, in an ice-water bath, 1.2 ml of a solution of *n*-butyllithium (1.1 M) were added. After 30 min. 400 µl (372.8 mg, 3.59 mmol) of $B(OMe)_3$ were added at once, and the reaction was allowed to proceed at room temperature for 1 h. On the side, a mixture of 128.1 mg (0.66 mmol) of 4-bromopyridine hydrochloride and 23.8 mg (0.021 mmol) of $Pd(PPh_3)_4$ in 3 ml of dry THF, degassed, under nitrogen, was stirred for 15 min. After this time, 5 drops of PEG 400, 3 ml of a degassed 2.5 M solution of K_2CO_3 and the previously prepared dithienylcyclopentene borate solution were added. The reaction was refluxed overnight. After addition of water and EtOAc, the layers were separated, and the organic phase was washed twice with water and once with brine. After drying with Na_2SO_4, filtering and solvent removing, **23** was obtained. Purification by flash chromatography using EtOAc as eluent yielded 48.2 mg (0.11 mmol, 47.8%).

^{1}H NMR (400 MHz, $CDCl_3$) δ: 8.57, (*d*, J=4.6, 4H), 7.28 (*bs*, 4H), 2.87-2.70 (*bm*, 4H), 2.31-2.04 (*m*, 14H); ^{13}C NMR (100 MHz, $CDCl_3$) δ: 149.9, 142.6, 138.0, 137.9, 135.6, 134.6, 131.4, 122.8, 37.7, 24.0, 15.4, 14.4. ESI-HRMS: 443.16215 $[M+H]^+$ (calc. for $C_{27}H_{27}N_2S_2^+$ 443.16102, Δm 2.55 ppm).

*Synthesis of 4,4'-(cyclopent-1-ene-1,2-diylbis(3,5-dimethylthiophene-4,2-diyl))bis(1-methylpyridin-1-ium) iodide (**1**)*

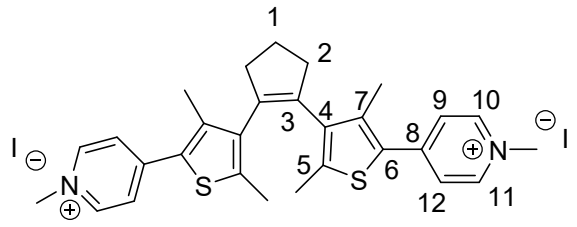

The previously obtained **23** (48.2 mg, 0.11 mmol) was dissolved in 3 ml of dry dichloromethane, under nitrogen. In an ice-water bath, 200 µl (456 mg, 3.21 mmol) of MeI were added and the reaction was allowed to proceed until total consumption of the starting material (overnight). After solvent removal and washing with diethyl ether, 58.1 mg (0.08 mmol, 72.7%) of **1** as an iodide salt were obtained.

^{1}H NMR (500 MHz, CD_3OD) δ: 8.70 (*bs*, 4H, H-9), 8.02, (*s*, 4H, H-10), 4.31 (*s*, 6H, *N*-CH_3), 2.98-2.73 (*bm*, 4H, H-2), 2.46 and 2.32 (*s*, 6H, 7-CH_3)*, 2.27-2.19 (*m*, 2H, H-1), 2.35 and 2.17 (*s*, 6H, 5-CH_3)*; ^{13}C NMR (125 MHz, CD_3OD) δ: 151.5 (C-8), 146.0 (C-10 and C-11), 143.9 and 143.7 (C-5)*$^{+}$, 142.8 and 142.7 (C-7)*, 141.2 and 141.1 (C-4)*$^{+}$, 140.0 and 140.0 (C-3)*, 130.1 (C-6), 125.6 (C-9 and C-12), 47.7 (*N*-CH_3), 38.9 and 38.8 (C-2)*, 24.9 (C-1), 17.0 (7-CH_3), 15.3 and 15.1 (5-CH_3)*; * in chemical exchange; $^{+}$ may be interchanged. ESI-HRMS: 236.10019 $[M]^{2+}$ (calc. for $C_{29}H_{32}N_2S_2^{2+}$ 236.09980, Δm 1.65 ppm); 457.17765 $[M\text{-}CH_3]^{+}$ (calc. for $C_{28}H_{29}N_2S_2^{+}$ 457.17667, Δm 2.14 ppm); 599.10587 $[M+I]^{+}$ (calc. for $C_{29}H_{32}IN_2S_2^{+}$ 599.10461, Δm 2.10 ppm).

*Synthesis of 2-chloro-5-methylthiophene (**14**)*

In a double neck flask under nitrogen, 75 ml of dry dichloromethane and 2.5 ml (2.54 g, 25.9 mmol) of 2-methylthiophene **12** were added. After cooling to 0 ºC, 2.3 ml (3.83 g,

28.4 mmol) of SO_2Cl_2 were cautiously added and the reaction was allowed to proceed for 35 min., time after which no starting material was present. The reaction mixture was poured into an ice-water bath, the layers were separated, and the aqueous phase was extracted twice with dichloromethane. After drying with Na_2SO_4, filtering and solvent removing, 2-chloro-5-methylthiophene **14** was obtained. The product was used in the following reaction without further purification.

^{1}H NMR (400 MHz, $CDCl_3$) δ: 6.69 (*d*, J=3.4, 1H), 6.52 (*s*, 1H), 2.41 (*s*, 3H).

*Synthesis of 1,5-bis(5-chloro-2-methylthiophen-3-yl)pentane-1,5-dione (**16**)*

To the previously prepared 2-chloro-5-methylthiophene **14** in 20 ml of dry dichloromethane, under nitrogen, 1.6 ml (2.12 g, 12.5 mmol) of glutaryl chloride were added. After cooling to 0 ºC, 5.19 g (39.0 mmol) of $AlCl_3$ were cautiously added, and the mixture was refluxed for 2 h 35 min, time after which no starting material was present. The crude was poured into an ice-water bath, the layers were separated, and the aqueous phase was extracted twice with dichloromethane. The gathered organic phases were dried with Na_2SO_4, filtered, and evaporated to afford the diketone **16**. The product was purified by dry column vacuum chromatography using mixtures of *n*-hexane/EtOAc – 9/1 and 8/2, to yield 2.48 g (6.87 mmol, 53.0% from **12**).

^{1}H NMR (400 MHz, $CDCl_3$) δ: 7.18 (*s*, 2H), 2.86 (*t*, J=6.8, 4H), 2.66 (*s*, 6H), 2.09-2.03 (*m*, 2H).

*Synthesis of 1,2-bis(5-chloro-2-methylthiophen-3-yl)cyclopent-1-ene (**18**)*

To a double neck flask with 1.06 g (16.2 mmol) of zinc dust and 20 ml of dry THF, degassed and under nitrogen, 1.3 ml (2.25 g, 11.9 mmol) of $TiCl_4$ were added at 0 ºC. The mixture was refluxed for 45 min, time after which 1.4 g (3.9 mmol) of the diketone **16** were added at 0 ºC, together with 5 ml of THF. The reaction was allowed to proceed at reflux until total consumption of the starting material (1 h 25 min). After cooling to 0 ºC, the reaction was quenched with a 10% K_2CO_3 solution and filtered through a pad of celite. The filtrate was dried over Na_2SO_4, filtered, and evaporated to yield dithienylcyclopentene **18**. Purification by dry column vacuum chromatography using *n*-hexane as eluent afforded 652.0 mg (1.98 mmol, 50.8%).

^{1}H NMR (400 MHz, $CDCl_3$) δ: 6.57 (*s*, 1H), 2.71 (*t*, J=7.4, 4H), 2.05-1.99 (*m*, 2H), 1.89 (*s*, 6H).

*Synthesis of 1,2-bis(2-methyl-5-(pyridin-4-yl)thiophen-3-yl)cyclopent-1-ene (**20**)*

To 109.1 mg (0.33 mmol) of the dithienylcyclopentene **18** in 5 ml of dry THF, degassed, under nitrogen, in an ice-water bath, 1.4 ml of a solution of *n*-buthyllithium (1.1 M) were added. After 30 min. 500 μl (466 mg, 4.49 mmol) of $B(OMe)_3$ were added at once, and the reaction was allowed to proceed at room temperature for 1 h. On the side, 26.8 mg (0.023 mmol) of $Pd(PPh_3)_4$ in 3 ml of dry THF, degassed, under nitrogen, were refluxed for 30 min. After this time 137.3 mg (0.71 mmol) of 4-bromopyridine hydrochloride, a catalytic amount of PEG 2000, 3 ml of a degassed 2.5 M solution of K_2CO_3, and the previously prepared dithienylcyclopentene borate solution were added. The reaction was refluxed overnight. After addition of water and EtOAc, the layers were separated, and the organic phase was washed twice with water and once with brine. After drying with

Na_2SO_4, filtering and solvent removing, **20** was obtained. Purification by flash chromatography using EtOAc and a mixture of EtOAc/MeOH - 9/1 as eluents yielded 85.3 mg (0.21 mmol, 63.6%).

^{1}H NMR (400 MHz, $CDCl_3$) δ: 8.53 (*d*, J=5.2, 4H), 7.34 (*d*, J=5.2, 4H) 7.21 (*s*, 2H) 2.85 (*t*, J=7.4, 4H), 2.15-2.07 (*m*, 2H), 2.02 (*s*, 6H).

*Synthesis of 4,4'-(cyclopent-1-ene-1,2-diylbis(5-methylthiophene-4,2-diyl))bis(1-methylpyridin-1-ium) iodide (**2**)*

To a solution of 13.1 mg (0.032 mmol) of **20** in 2 ml of dry dichloromethane, under nitrogen, in an ice-water bath, 20 μl (45.6 mg, 0.32 mmol) of MeI were added. The reaction was allowed to proceed at room temperature for 3h30min, time after which another 20 μl (45.6 mg, 0.32 mmol) of MeI were added. The reaction was allowed to procced until total consumption of the starting material, time after which the solvent was evaporated to dryness. The crude was washed with diethyl ether, yielding 13.3 mg (0.019 mmol, 59.4%) of **2** as an iodide salt.

^{1}H NMR (400 MHz, $CDCl_3$) δ: 8.83 (*d*, J=6.2, 4H), 7.97 (*d*, J=6.6, 4H) 7.54 (*s*, 2H) 4.39 (*s*, 6H), 2.88-2.84 (*m*, 4H), 2.34 (*s*, 6H), 2.04 (*m*, 2H).

*Synthesis of 1,2-bis(2-methyl-5-(pyridin-3-yl)thiophen-3-yl)cyclopent-1-ene (**21**)*

To 104.9 mg (0.32 mmol) of the dithienylcyclopentene **18** in 5 ml of dry THF, degassed, under nitrogen, in an ice-water bath, 1.4 ml of a solution of *n*-buthyllithium (1.1 M) were added. After 30 min. 500 μl (466 mg, 4.49 mmol) of $B(OMe)_3$ were added at once, over ice, and the reaction was allowed to proceed at room temperature for 1 h. On the side,

28.3 mg (0.025 mmol) of $Pd(PPh_3)_4$ in 3 ml of dry THF, degassed, under nitrogen, were refluxed for 30 min. After this time 3 ml of a 2.5 M solution of K_2CO_3, 5 drops of PEG 400, 80 µl (131.2 mg, 0.83 mmol) of 3-bromopyridine and the previously prepared dithienylcyclopentene borate solution were added. The reaction was refluxed overnight. After addition of water and EtOAc, the layers were separated and the organic phase was washed twice with water and once with brine. After drying with Na_2SO_4, filtering and solvent removing, **21** was obtained. Purification by flash chromatography using EtOAc as eluent yielded 51.2 mg (0.12 mmol, 37.5% corrected by NMR), contaminated with Ph_3PO. NMR spectra were subtracted with an authentic sample of Ph_3PO and the compound was used in the following step without further purification.

^{1}H NMR (400 MHz, $CDCl_3$) δ: 8.76 (*s*, 2H), 8.45 (*d*, J=3.7, 2H), 7.73 (*d*, J=7.8, 2H), 7.26 (*overlapped with $CHCl_3$*), 7.06 (*s*, 2H), 2.86 (*t*, J=7.4,4H), 2.14-2.09 (m, 2H), 2.04 (*s*, 6H); ^{13}C NMR (100 MHz, $CDCl_3$) δ: 148.0, 146.5, 136.9, 135.9, 135.8, 134.8, 132.3, 130.4, 125.1, 123.6, 38.4, 23.0, 14.5. ESI-HRMS: 415.13246 $[M+H]^+$ (calc. for $C_{25}H_{23}N_2S_2^+$ 415.12972, Δm 6.60 ppm).

*Synthesis of 3,3'-(cyclopent-1-ene-1,2-diylbis(5-methylthiophene-4,2-diyl))bis(1-methylpyridin-1-ium) iodide (**3**)*

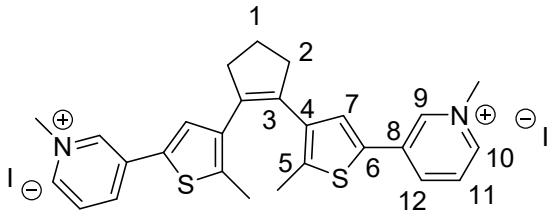

To the previously prepared **21** (70.9 mg, 0.17 mmol) in 3 ml of dry dichloromethane, under nitrogen, in an ice-water bath, 200 µl (456 mg, 3.21 mmol) of MeI were added. The

reaction was allowed to proceed at room temperature until total consumption of the starting material, time after which the solvent was evaporated to dryness. The crude was washed with diethyl ether, yielding 79.5 mg (0.11 mmol, 64.7%) of **3** as an iodide salt. The product was recrystalized from a mixture of dichloromethane/methanol and diethyl ether.

^{1}H NMR (500 MHz, CD_3OD) δ: 9.23 (*s*, 2H, H-9), 8.69 (*d*, J=5.5, 2H, H-10), 8.63 (*d*, J=8.2, 2H, H-12), 8.01 (*t*, J=6.9, 2H, H-11), 7.68 (*s*, 2H, H-7), 4.43 (*s*, 6H, *N*-CH_3), 2.92 (*t*, J=7.1, 4H, H-2), 2.20-2.14 (*m*, 2H, H-1), 2.06 (*s*, 6H, 5-CH_3); ^{13}C NMR (125 MHz, CD_3OD) δ: 143.7 (C-10), 142.8 (C-9), 141.1 (C-12), 140.9 (C-5), 139.4 (C-4), 136.5* (C-3), 136.4* (C-8), 132.8 (C-6), 130.4 (C-7), 129.2 (C-11), 49.2^{+} (*N*-CH_3), 39.6 (C-2), 24.0 (C-1), 14.7 (5-CH_3); * may be interchanged; $^{+}$ determined by DEPT-135. ESI-HRMS: 222.08469 $[M]^{2+}$ (calc. for $C_{27}H_{28}N_2S_2^{2+}$ 222.08415, Δm 2.43 ppm); 429.14682 $[M\text{-}CH_3]^{+}$ (calc. for $C_{26}H_{25}N_2S_2^{+}$ 429.14537, Δm 3.38 ppm); 571.07475 $[M+I]^{+}$ (calc. for $C_{27}H_{28}IN_2S_2^{+}$ 571.07331, Δm 2.52 ppm).

*Synthesis of 1,2-bis(2-methyl-5-(pyridin-2-yl)thiophen-3-yl)cyclopent-1-ene (**22**)*

To 117.8 mg (0.36 mmol) of the dithienylcyclopentene **18** in 5 ml of dry THF, degassed, under nitrogen, in an ice-water bath, 1.4 ml of a solution of *n*-buthyllithium (1.1 M) were added. After 30 min. 500 μl (466 mg, 4.49 mmol) of $B(OMe)_3$ were added at once, and the reaction was allowed to proceed at room temperature for 1 h. On the side, 27.8 mg (0.024 mmol) of $Pd(PPh_3)_4$ in 3 ml of dry THF, degassed, under nitrogen, were refluxed for 30 min. After this time 3 ml of a 2.5 M solution of K_2CO_3, 5 drops of PEG 400, 80 μl (132.6 mg, 0.84 mmol) of 2-bromopyridine and the previously prepared dithienylcyclopentene borate solution were added. The reaction was refluxed overnight.

After addition of water and EtOAc, the layers were separated and the organic phase was washed twice with water and once with brine. After drying with Na_2SO_4, filtration and solvent removal, **22** was obtained. Purification by flash chromatography using a mixture of *n*-hexane/EtOAc - 8/2 as eluent yielded 76.4 mg (0.18 mmol, 50.0%).

^{1}H NMR (400 MHz, $CDCl_3$) δ: 8.51 (*d*, J=4.3, 2H), 7.61 (*t*, J=7.6, 2H), 7.50 (*d*, J=8.0, 2H), 7.32 (*s*, 2H), 7.08 (*s*, J=6.0, 2H), 2.86 (*t*, J=7.4,4H), 2.12-2.07 (m, 2H), 2.02 (*s*, 6H); ^{13}C NMR (100 MHz, $CDCl_3$) δ: 152.6, 149.4, 140.1, 137.6, 136.8, 136.5, 134.6, 125.6, 121.4, 118.4, 38.5, 23.0, 14.7.

*Synthesis of 2,2'-(cyclopent-1-ene-1,2-diylbis(5-methylthiophene-4,2-diyl))bis(1-methylpyridin-1-ium) iodide (**4**)*

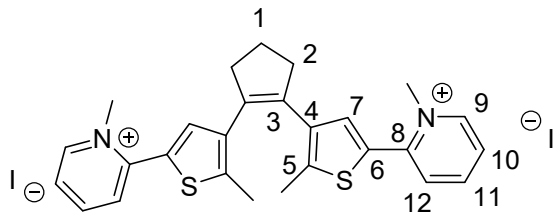

To 42.0 mg (0.10 mmol) of **22** in 4 ml of dry acetonitrile 200 µl of MeI were added. The reaction was allowed to proceed in a closed vessel for 3 days, time after which another 200 µl of MeI were added. After another 4 days, and disappearance of the starting material, the solvent was evaporated to dryness and the crude was thoroughly washed with diethyl ether, yielding 62.3 mg (0.089 mmol, 89.0%) of **4**. The product was recrystalized from a mixture of dichloromethane/methanol and diethyl ether.

^{1}H NMR (500 MHz, CD_3OD) δ: 8.93 (*d*, J=5.6, 2H, H-9), 8.51 (*t*, J=7.8, 2H, H-11)), 8.15 (*d*, J=8.0, 2H, H-12), 7.96 (*t*, J=6.5, 2H, H-10), 7.56 (*s*, 2H, H-7), 4.35 (*s*, 6H, *N*-CH_3), 2.94 (*t*, J=7.4, 4H, H-2), 2.25 (*s*, 6H, 5-CH_3), 2.21-2.16 (*m*, 2H, H-1); ^{13}C NMR (125

MHz, CD_3OD) δ: 150.9 (C-8), 148.3 (C-9), 146.3 (C-11), 144.1* (C-5), 138.8* (C-4), 137.0 (C-3), 136.5 (C-7), 131.5 (C-12), 128.7 (C-6), 127.1 (C-10), 48.9$^+$ (*N*-CH_3), 39.2 (C-2), 24.1 (C-1), 14.6 (5-CH_3); * may be interchanged; $^+$ determined by DEPT-135. ESI-HRMS: 222.08468 $[M]^{2+}$ (calc. for $C_{27}H_{28}N_2S_2^{2+}$ 222.08415, Δm 2.39 ppm); 429.14730 $[M\text{-}CH_3]^+$ (calc. for $C_{26}H_{25}N_2S_2^+$ 429.14537, Δm 4.50 ppm); 571.07529 $[M+I]^+$ (calc. for $C_{27}H_{28}IN_2S_2^+$ 571.07331, Δm 3.47 ppm).

3. Indicator displacement assays

Binding constants were determined from indicator displacement assays using following set of coupled equations:

$$A_{obs} = \varepsilon^I[I] + \varepsilon^C[IC] = \varepsilon^I[I] + \varepsilon^C[I]_0 - \varepsilon^C[I] = \varepsilon^C[I]_0 + (\varepsilon^I - \varepsilon^C)[I] \qquad (2)$$

Equation 2 assumes that only the free and complexed dye absorbs at the monitorization wavelength (*i.e.*, the guest competitor does not absorb either as a free or complexed species). [I] and [IC] are the *equilibrium* concentrations of free and complexed indicator dye, respectively, while $[I]_0$ =[I] + [IC] is the total concentration of indicator. ε^I and ε^C are the molar extinction coefficients of free and complexed indicator at the monitorizations wavelength.

According to the mass balance and equilibrium expressions the following equations can be written:

$$K_I = \frac{[IC]}{[I][CB8]} \quad (3) \qquad K_G = \frac{[GC]}{[G][CB8]} \quad (4)$$

$$[I]_0 = [IC] + [I] = K_I[I][CB8] + [I] \qquad (5)$$

$$[G]_0 = [GC] + [G] = K_G[G][CB8] + [G] \qquad (6)$$

$$[CB8]_0 = [GC] + [IC] + [CB8] = K_G[G][CB8] + K_I[I][CB8] + [CB8] \qquad (7)$$

and combined to give equations 8-10:

$$[I] = \frac{[I]_0}{1 + K_I[CB8]} \qquad (8)$$

$$[G] = \frac{[G]_0}{1 + K_G[CB8]} \qquad (9)$$

$$A[CB8]^3 + ; B[CB8]^2 + C[CB8] - [CB8]_0 = 0 \qquad (10)$$

$$A = K_G K_I$$

$$B = K_G K_I([G]_0 + [I]_0 - [CB8]_0) + K_G + K_I$$

$$C = K_G([G]_0 - [CB8]_0) + K_I([I]_0 - [CB8]_0) + 1$$

The experimental data can be fitted to equation 11 (using solver tool in an Excel spreadsheet for example) coupled with the cubic equation 10 that can be solved using the Newton-Raphson algorithm. In indicator displacement assays one of the binding constants is usually known and used as reference and kept constant (K_I or K_G) while the other can be optimized through data fitting.

$$A_{obs} = \frac{(\varepsilon^I - \varepsilon^C)[I]_0}{1 + K_I[CB8]} + \varepsilon^C[I]_0 \qquad (11)$$

When performing these titrations, it is important to select competitors that form clean 1:1 complex with CB8, avoiding the formation of heteroternary, homoternary or higher order complexes, and ensure that the DTE is not present as mixture of isomers. For the open form this can be straightforwardly verified by the absence of absorption bands in their

UV-Vis spectra at wavelengths > 500 nm. For the closed forms this verification must be performed before the titration experiments, through the determination of the photostationary state composition using techniques, such as ^{1}H NMR or HPLC. For all compounds studied herein, the open isomers can be quantitatively formed by irradiation at λ_{irr} > 500 nm while the closed isomers are formed with conversion yields ≥ 95% through irradiation at λ_{irr} = 365 nm in the presence of CB8.

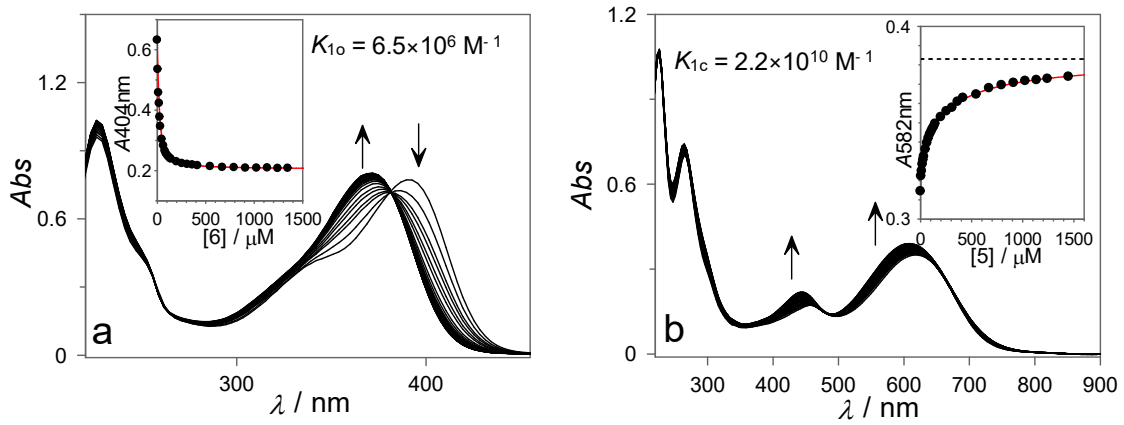

Figure S1 –(a) Spectral changes observed upon addition of **6** to a solution containing equimolar concentrations of **1o**:CB8 (23 μM in H_2O). (b) The same for the addition of **5** to **1c**:CB8 (30 μM in H_2O). The dotted line represents the limiting absorbance estimated for free **1c**.

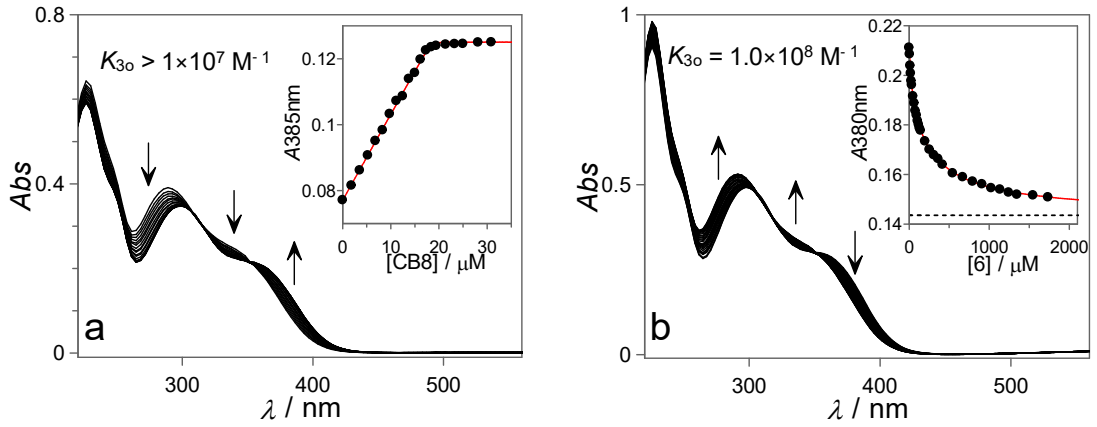

Figure S2 – (a) Spectral changes observed upon gradual addition of CB8 to a solution of **3o** (18 μM in H_2O). (b) Spectral changes observed addition of **6** to a solution containing equimolar concentrations of **3o**:CB8 (26 μM in H_2O). The dotted line represents the limiting absorbance estimated for free **3o**.

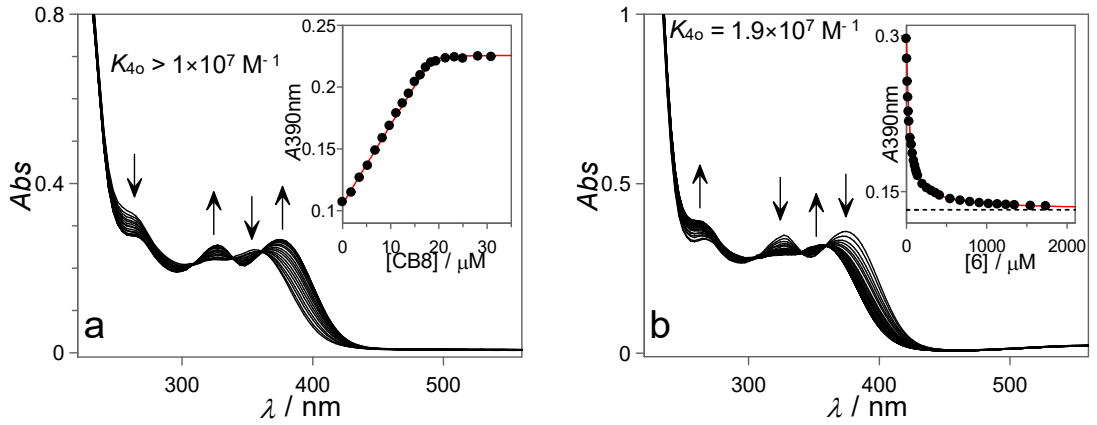

Figure S3 – (a) Spectral changes observed upon gradual addition of CB8 to a solution of **4o** (19 μM in H_2O). (b) Spectral changes observed addition of **6** to a solution containing equimolar concentrations of **4o**:CB8 (24 μM in H_2O). The dotted line represents the limiting absorbance estimated for free **4o**.

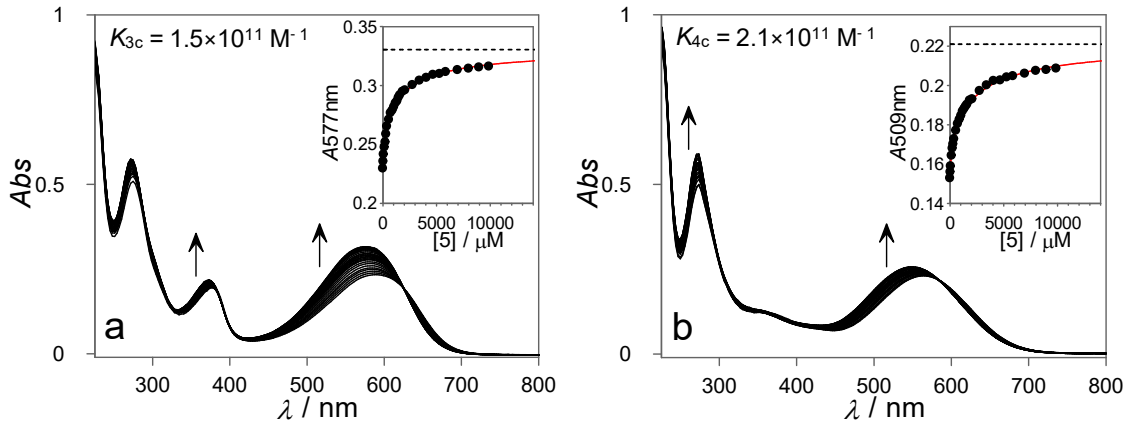

Figure S4 – (a) Spectral changes observed upon addition of **5** to a solution containing equimolar concentrations of **3c**:CB8 (25 μM in H_2O). (b) The same for the addition of **5** to **4c**:CB8 (27 μM in H_2O). The dotted line represents the limiting absorbance estimated for free **3c/4c**.

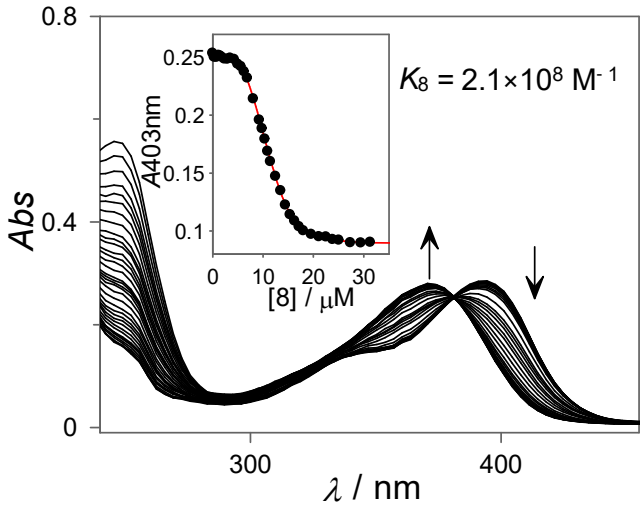

Figure S5 –Spectral changes observed upon addition of testosterone **8** to a solution containing **1o** (9 μM in H_2O) and CB8 (15 μM in H_2O). The concentration of **1o** and CB8 was kept constant throughout the titration.

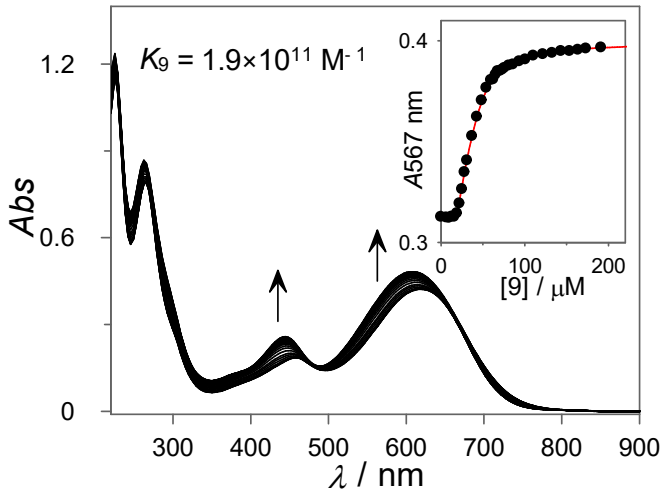

Figure S6 –Spectral changes observed upon addition of vecuronium **9** to a solution containing **1c** (32 μM in H_2O) and CB8 (50 μM in H_2O). The concentration of **1c** and CB8 was kept constant throughout the titration.

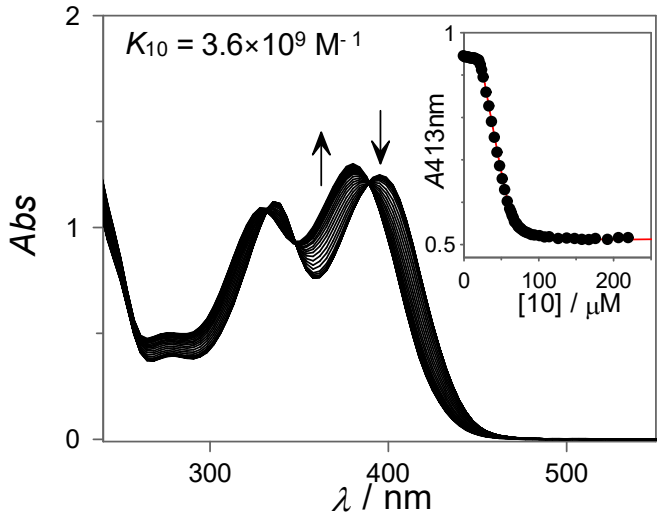

Figure S7 –Spectral changes observed upon addition of pancuronium **10** to a solution containing **2o** (43 μM in H_2O) and CB8 (65 μM in H_2O). The concentration of **2o** and CB8 was kept constant throughout the titration.

4. ITC titrations

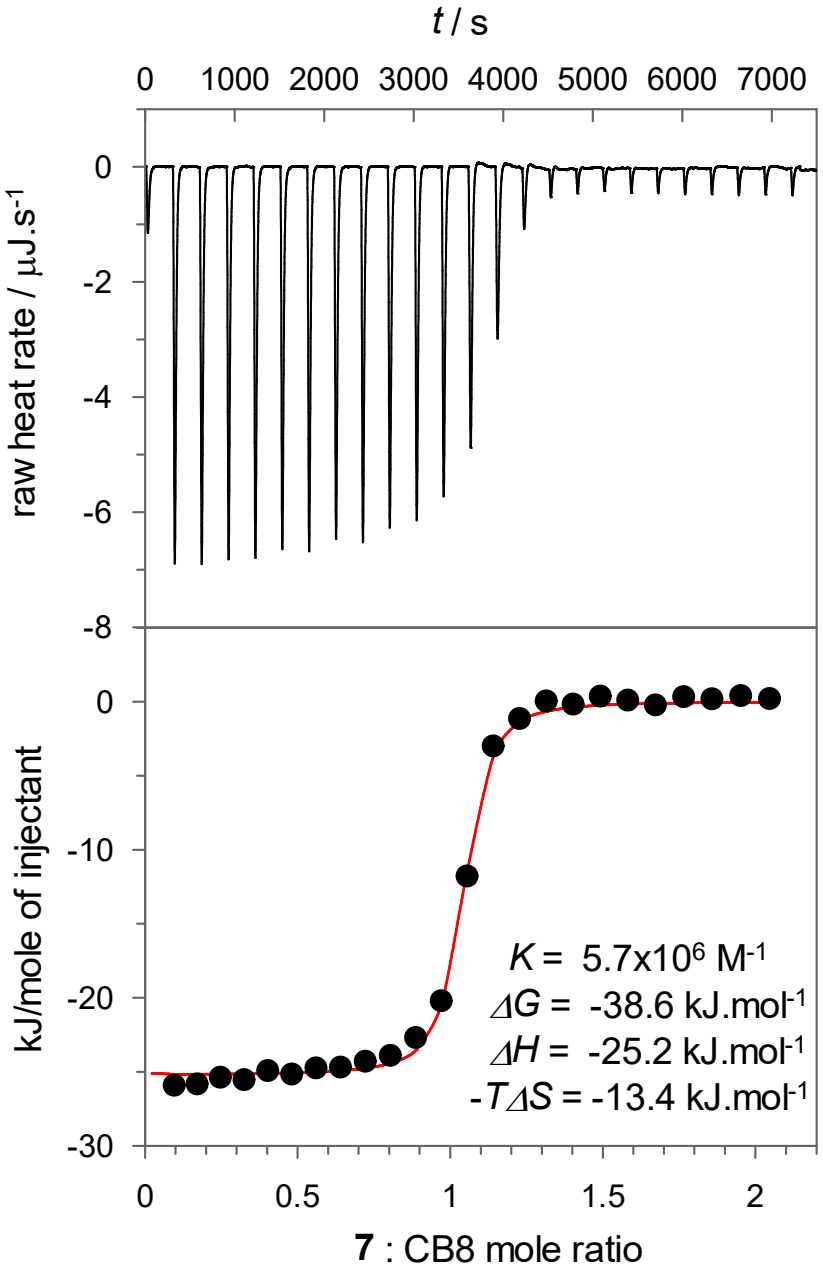

Figure S8 –Isotherm for the titration of methyl viologen **7** (0.72 mM) into CB8 (0.10 mM) in water at 25 ºC.

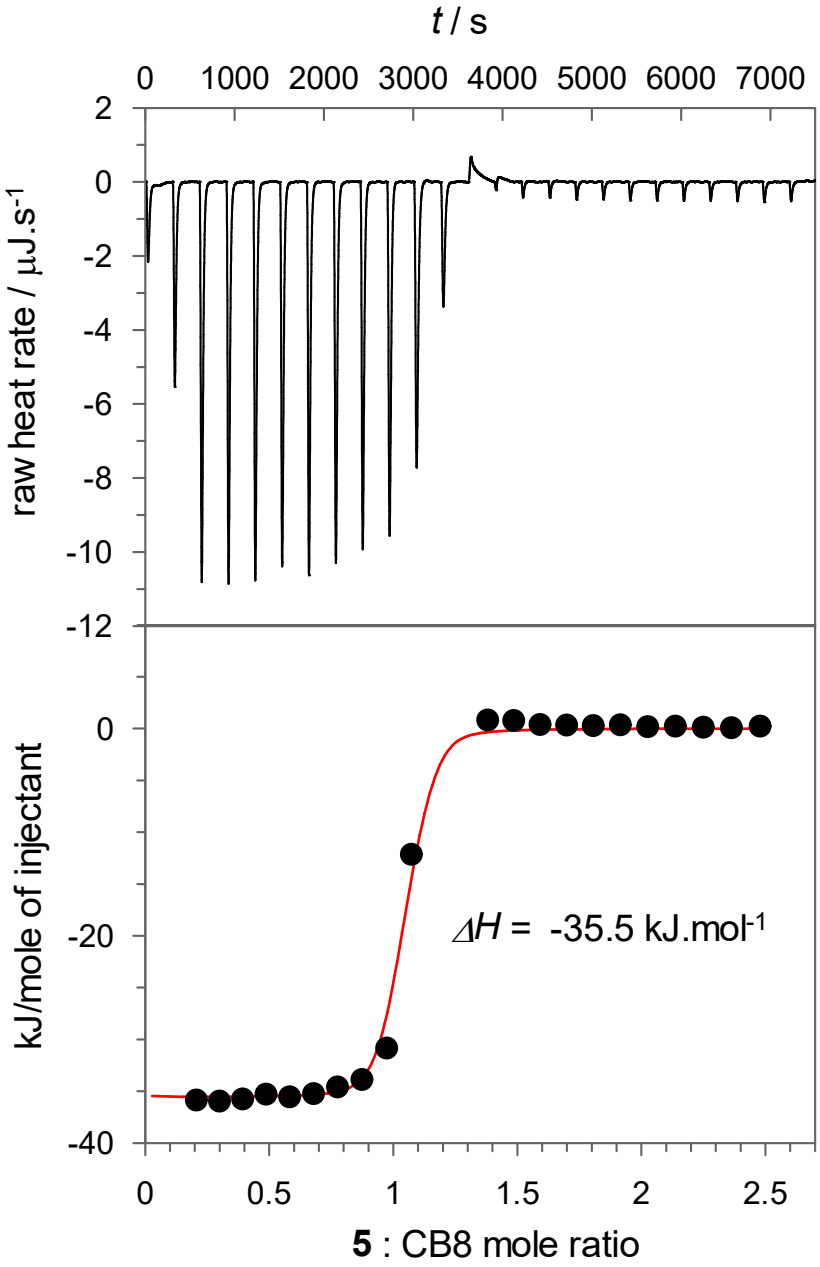

Figure S9 –Isotherm for the titration of 1-adamantyl ammonium **5** (0.90 mM) into CB8 (0.10 mM) in water at 25 ºC.

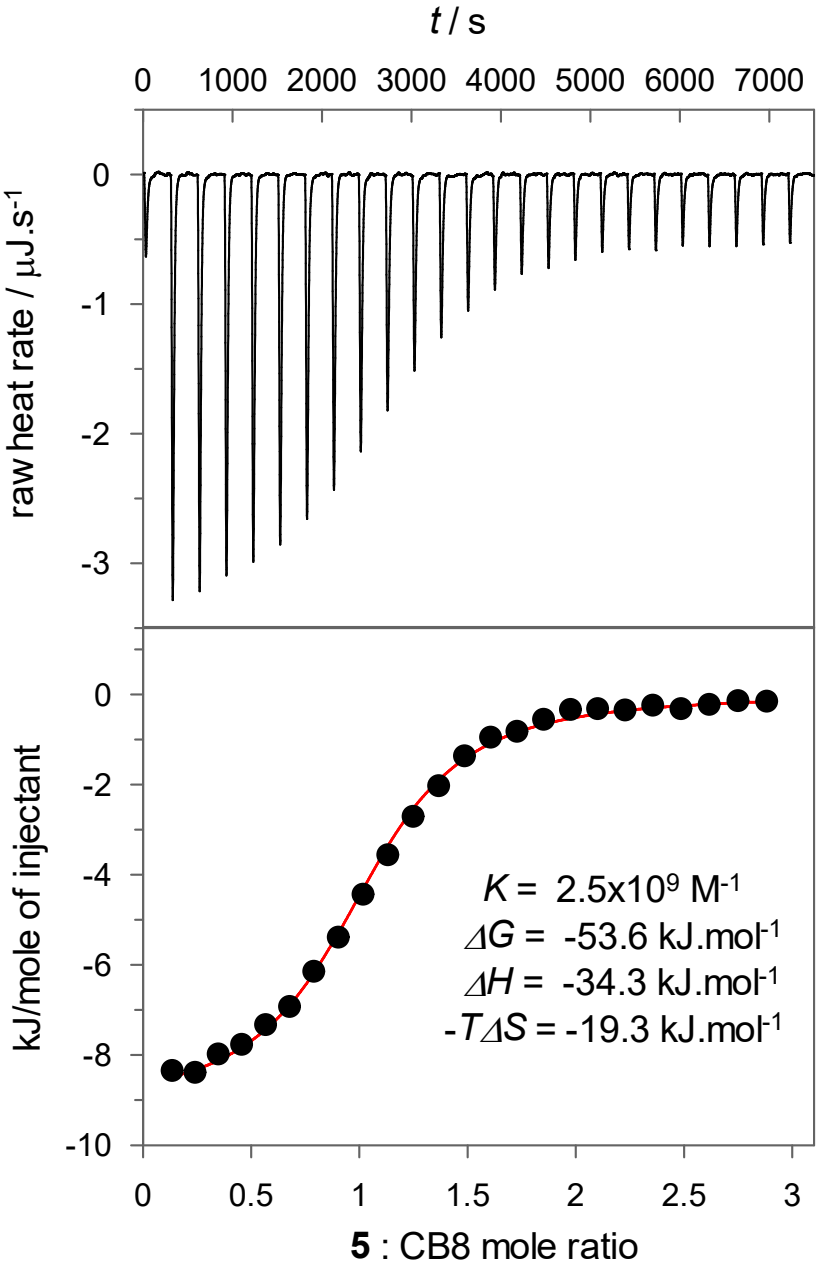

Figure S10 –Isotherm for the competitive titration of 1-adamantyl ammonium **5** (1.00 mM) into a CB8 solution (0.10 mM) containing 3.00 mM of methyl viologen **7**. The titration was performed in water at 25 ºC. The data fitting was achieve using a competitive replacement model with the CB8:**7** binding constant (K_7 = 5.7×10^6 M^{-1}) and enthalpy variation (ΔH = –25.2 kJ.mol^{-1}) set as constants.

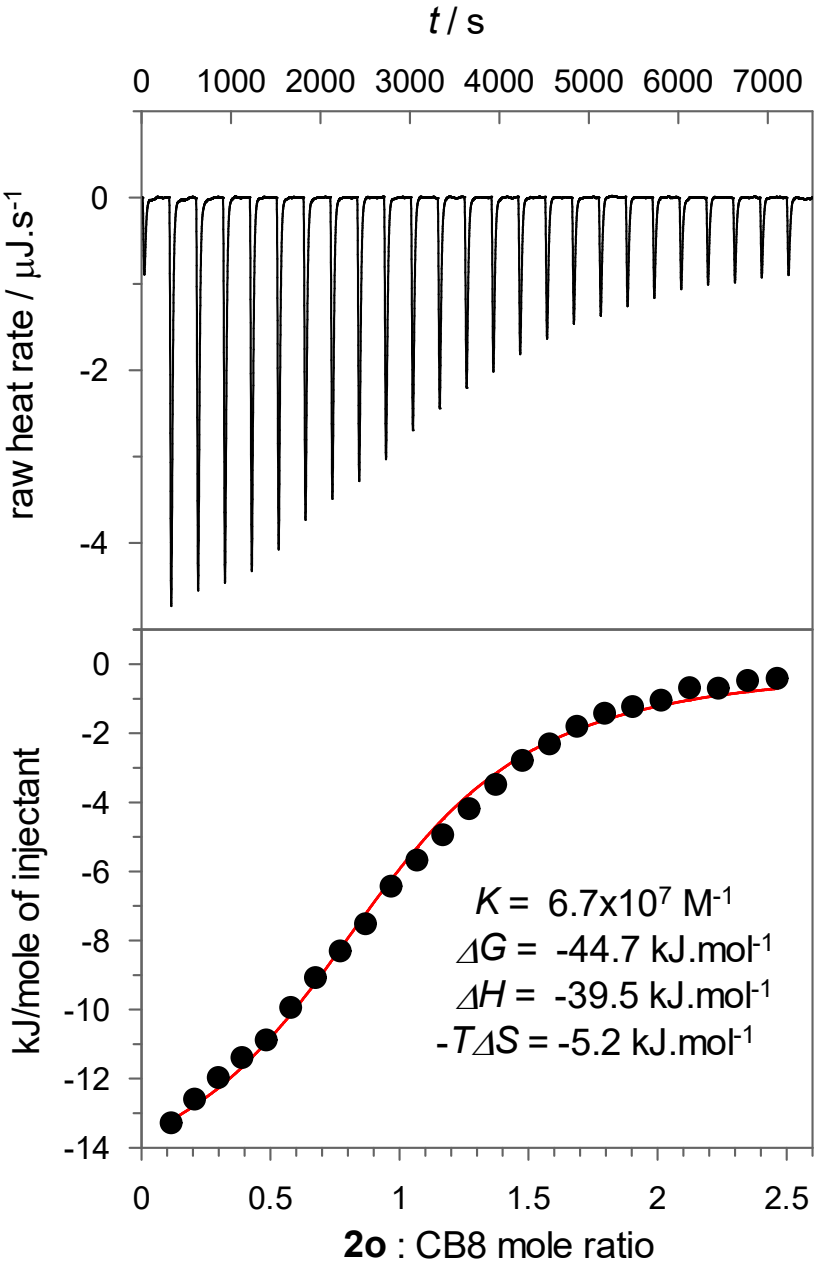

Figure S11 –Isotherm for the competitive titration of DTE **2o** (0.94 mM) into a CB8 solution (0.11 mM) containing 0.20 mM of methyl viologen **7**. The titration was performed in water at 25 ºC. The data fitting was achieve using a competitive replacement model with the CB8:**7** binding constant (K_7 = 5.7×10^6 M^{-1}) and enthalpy variation (ΔH = –25.2 kJ.mol^{-1}) set as constants.

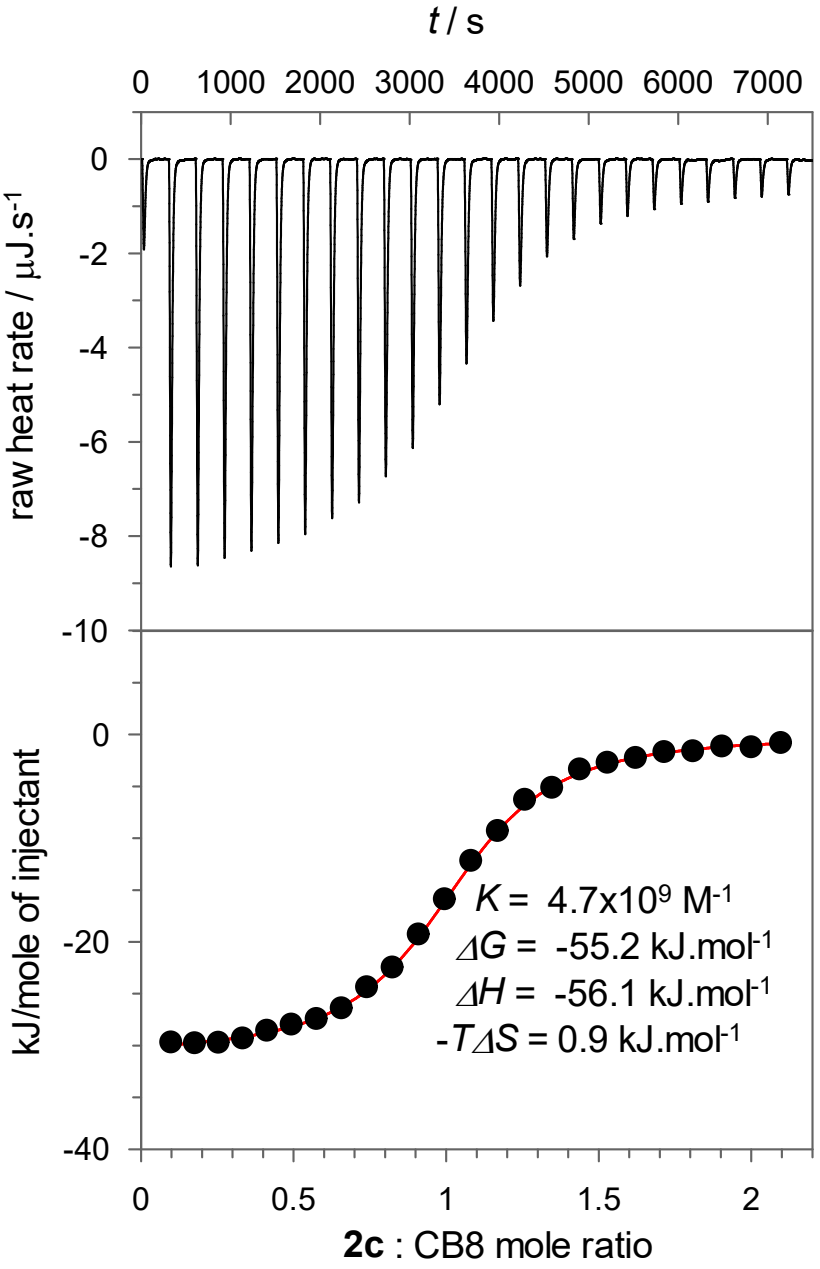

Figure S12 –Isotherm for the competitive titration of DTE **2c** (0.80 mM) into a CB8 solution (0.11 mM) containing 3.00 mM of methyl viologen **7**. The titration was performed in water at 25 ºC. The data fitting was achieve using a competitive replacement model with the CB8:**7** binding constant (K_7 = 5.7×10^6 M^{-1}) and enthalpy variation (ΔH = –25.2 kJ.mol^{-1}) set as constants.

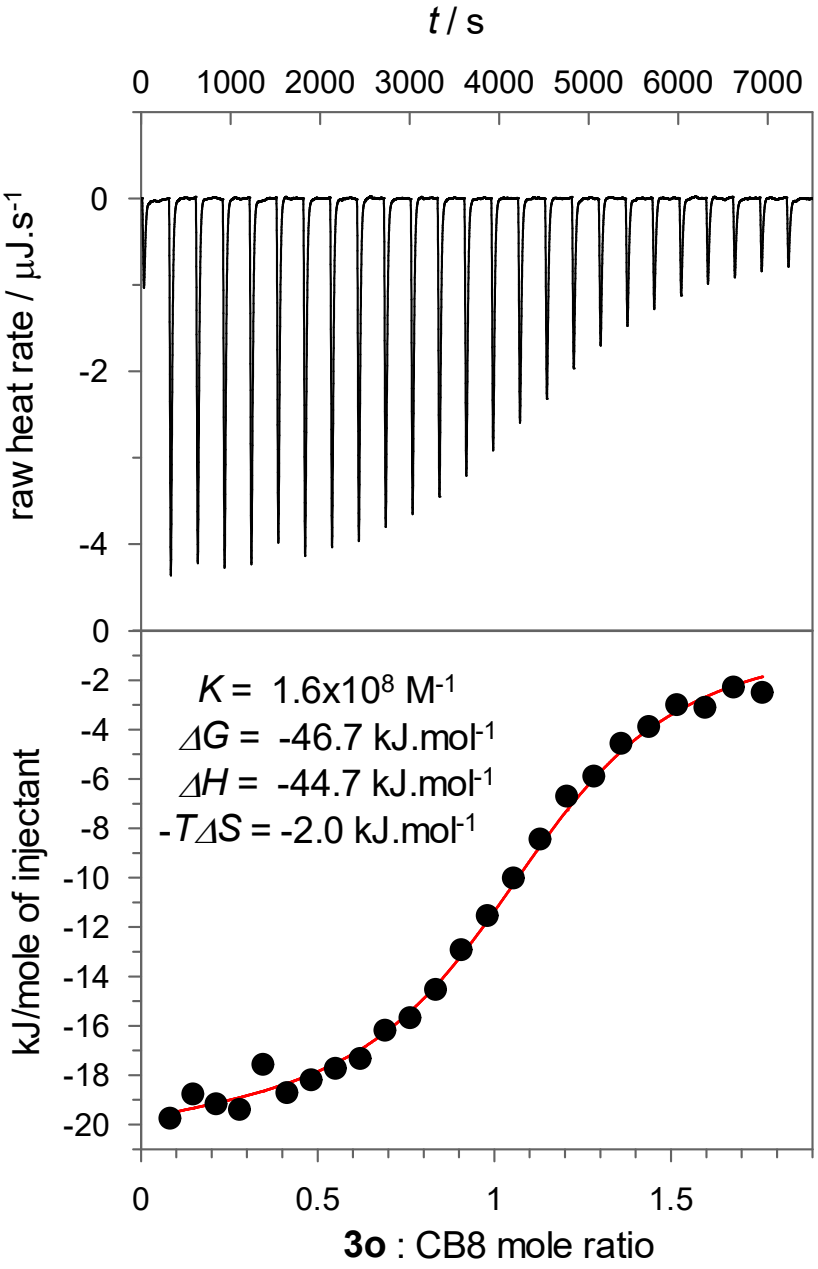

Figure S13 –Isotherm for the competitive titration of DTE **3o** (0.60 mM) into a CB8 solution (0.10 mM) containing 0.15 mM of methyl viologen **7**. The titration was performed in water at 25 ºC. The data fitting was achieve using a competitive replacement model with the CB8:**7** binding constant (K_7 = 5.7×10^6 M^{-1}) and enthalpy variation (ΔH = –25.2 kJ.mol^{-1}) set as constants.

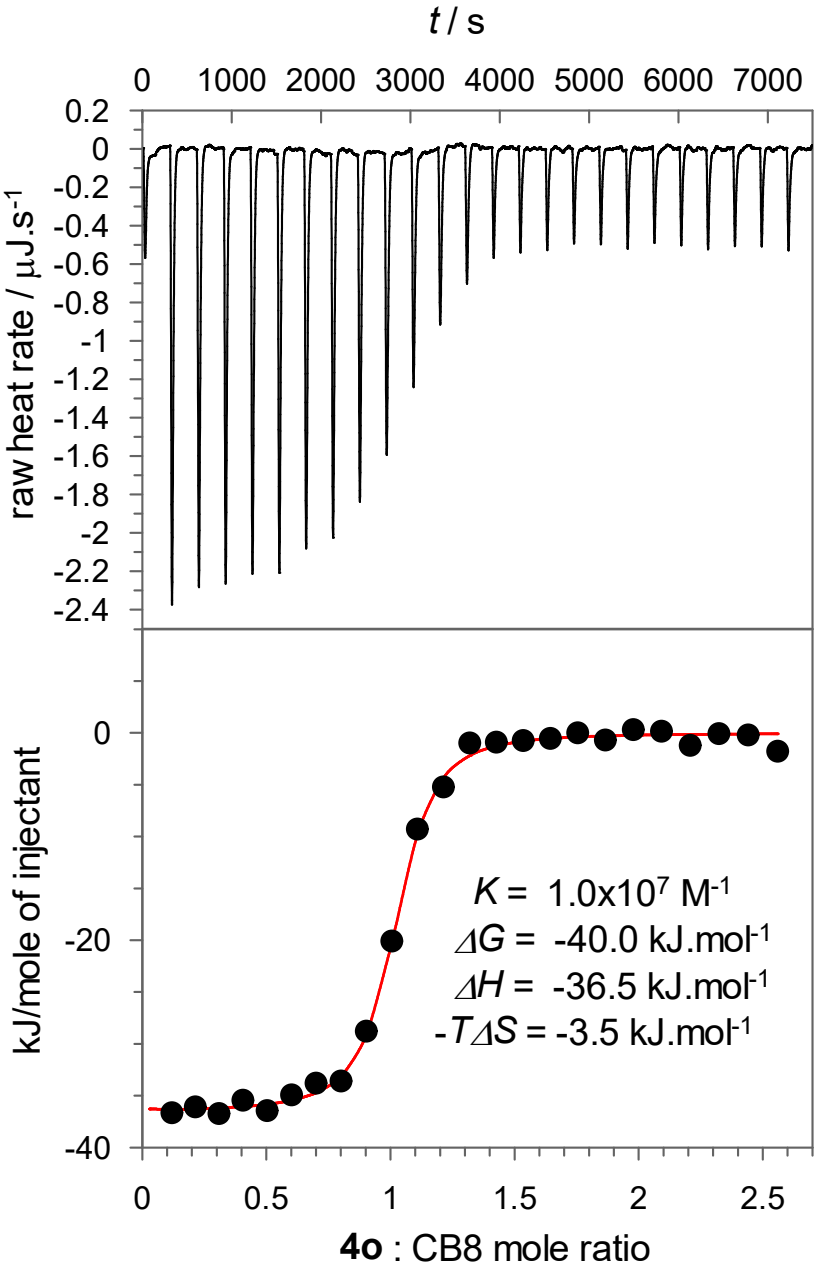

Figure S14 –Isotherm for the titration of DTE **4o** (0.15 mM) into CB8 (0.017 mM) in water at 25 ºC.

5. Computational Details

Conformational Space Sampling. Initial structures of each CB8:DTE host:guest system, featuring both antiparallel-open (**o**) and closed (**c**) guests, were manually built by placing the DTE guest molecules inside the CB8 host. Then, an automated exploration of the chemical space was performed using the Conformer-Rotamer Ensemble Sampling Tool (CREST Version 2.11)[8] by applying an iterative meta-dynamics with genetic crossing (iMTD-GC) algorithm[9] along with the GFN2-xTB tight-binding semiempirical method[10] as implemented in xtb-6.4.0.[11] Default parameters were employed for the CREST/iMTD-GC procedure and in accordance, an ensemble of conformers and rotamers within a 6 kcal mol^{-1} energy window, optimized with very tight thresholds in implicit water with the analytical linearized Poisson-Boltzmann (ALPB) model, are obtained.

DFT calculations and electrostatic potential analysis. For each host:guest system, and in accordance with the NMR results, the fully inserted lowest-energy structure was selected for further optimization with the ωB97X-D functional, which uses a version of Grimme's D2 dispersion model[12] and a standard 6-31G* basis set in Gaussian 09.[13] Solvent effects (water) were included implicitly using the SMD variation of the integral equation formalism variant (IEFPCM).[14]

The analysis of the electrostatic potential and extrema calculation, in particular, the evaluation of maxima associated with the sulfur atoms corresponding to the σ-holes (V_{max}) was performed with Multiwfn Version 3.8[15] on optimized structures at the ωB97X-D/6-31G* level of theory. For extrema analysis and representations purposes, the electrostatic potential is mapped on the 0.004 au contour of the electron density.

Analysis of the intermolecular noncovalent interactions. The analysis of noncovalent interactions was performed with IGMPlot Rev. 2.6.9b.[16] This is based on the Independent

Gradient Model,[17,18] more specifically on the electron density-based descriptor IGM-δg^{inter}. The model can quantify the net electron density gradient attenuation due to molecular interactions and hence, by using an uncoupling scheme, δg^{inter} uniquely defines intermolecular interaction regions. In this work, the electron density was derived from the wave function generated from the DFT calculations using the Gradient-Based Partitioning (GBP) scheme.[17] Plotting δg^{inter} isosurfaces, colored according to the sign of the second eigenvalue of the electron density hessian matrix (λ_2), allows to differentiate between non-bonding ($\lambda 2>0$) from attractive ($\lambda 2<0$) interactions. In practice, a BGR color code is commonly used: red for strongly repulsive, green for van der Waals, and blue for strongly attractive interactions.

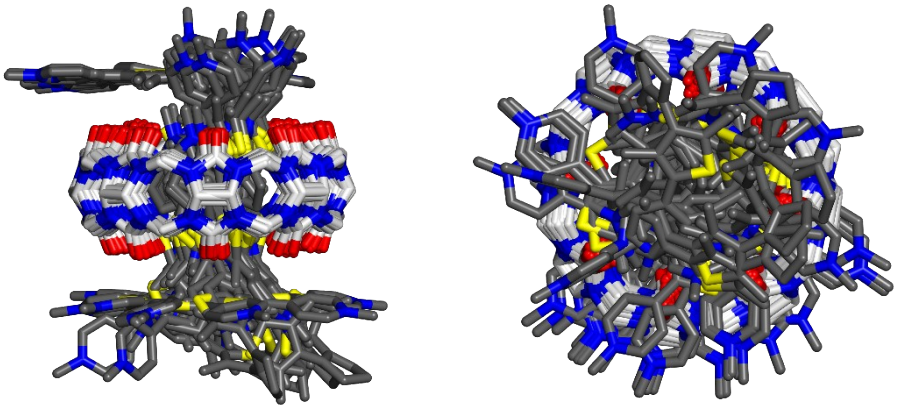

CB8:**1o** (nconfs = 58)

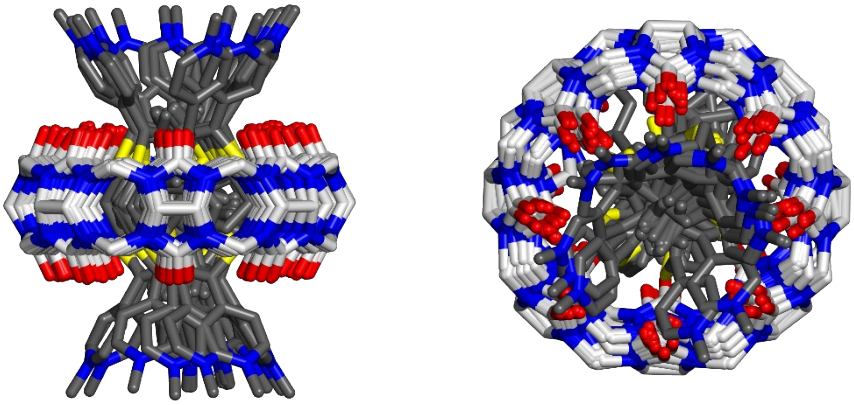

CB8:**1c** (nconfs = 17)

Figure S15 – Ensemble of lowest-energy conformers (nconfs is the number of conformations) within 6 kcal mol^{-1} above the lowest conformer, generated by CREST at the GFN2-xTB level for host:guest systems CB8:**1o** and CB8:**1c** employing the ALPB model for solvation in water. The structures were fitted for the CB8 host.

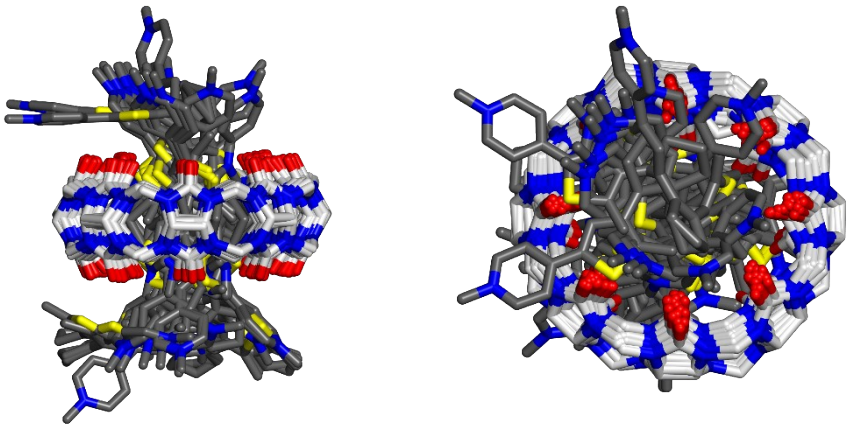

CB8:**2o** (nconfs = 27)

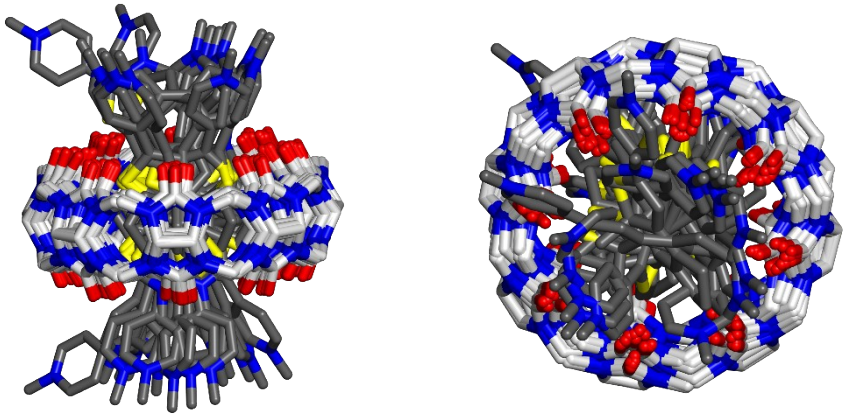

CB8:**2c** (nconfs = 18)

Figure S16 – Ensemble of lowest-energy conformers (nconfs is the number of conformations) within 6 kcal mol^{-1} above the lowest conformer, generated by CREST at the GFN2-xTB level for host:guest systems CB8:**2o** and CB8:**2c** employing the ALPB model for solvation in water. The structures were fitted for the CB8 host.

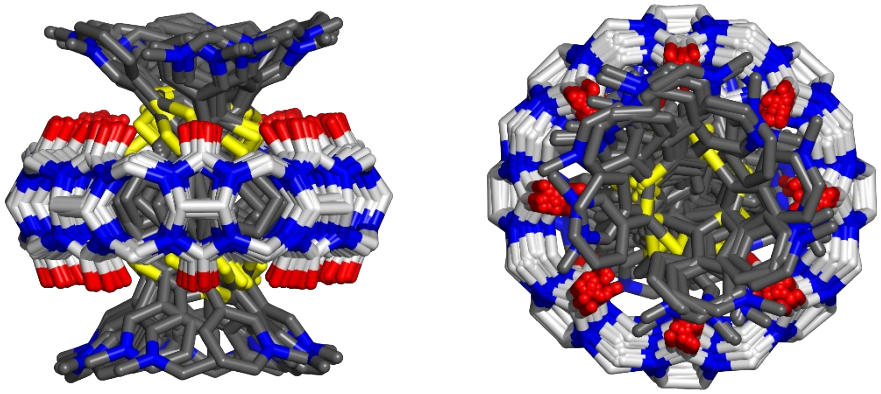

CB8:**3o** (nconfs = 28)

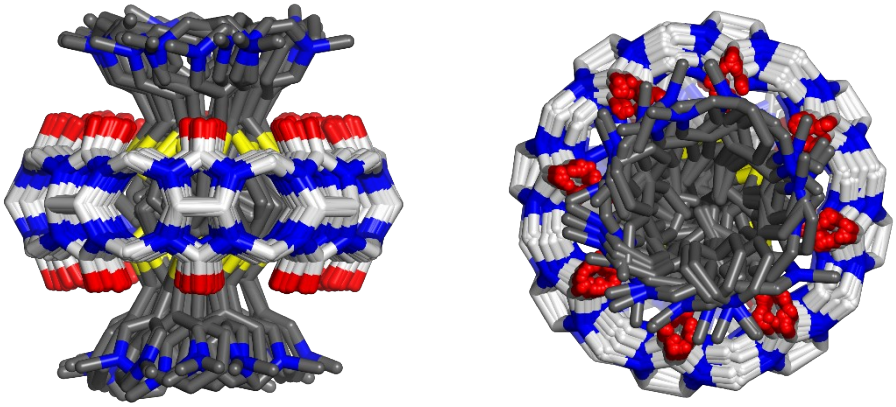

CB8:**3c** (nconfs = 34)

Figure S17 – Ensemble of lowest-energy conformers (nconfs is the number of conformations) within 6 kcal mol^{-1} above the lowest conformer, generated by CREST at the GFN2-xTB level for host:guest systems CB8:**3o** and CB8:**3c** employing the ALPB model for solvation in water. The structures were fitted for the CB8 host.

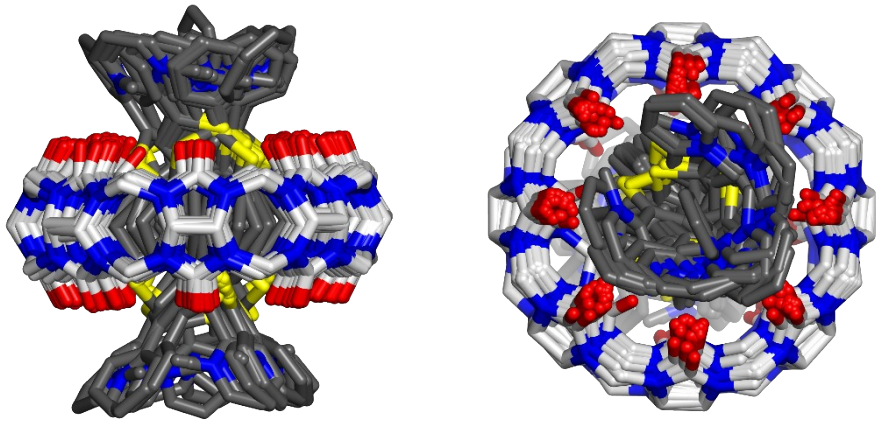

CB8:**4o** (nconfs = 27)

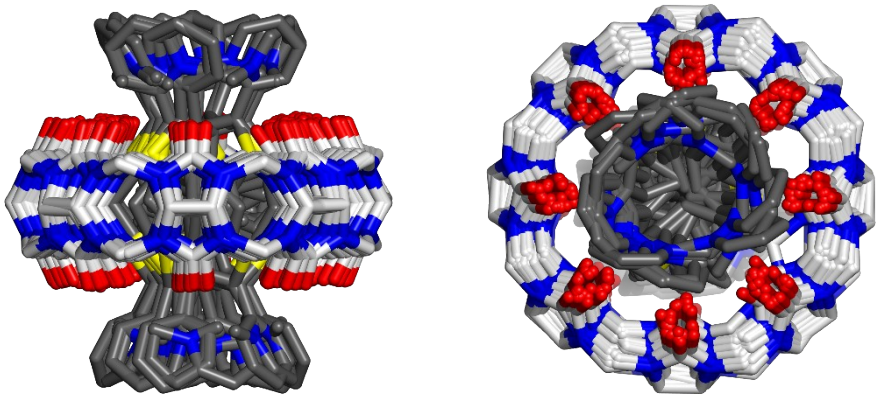

CB8:**4c** (nconfs = 28)

Figure S18 – Ensemble of lowest-energy conformers (nconfs is the number of conformations) within 6 kcal mol^{-1} above the lowest conformer, generated by CREST at the GFN2-xTB level for host:guest systems CB8:**4o** and CB8:**4c** employing the ALPB model for solvation in water. The structures were fitted for the CB8 host.

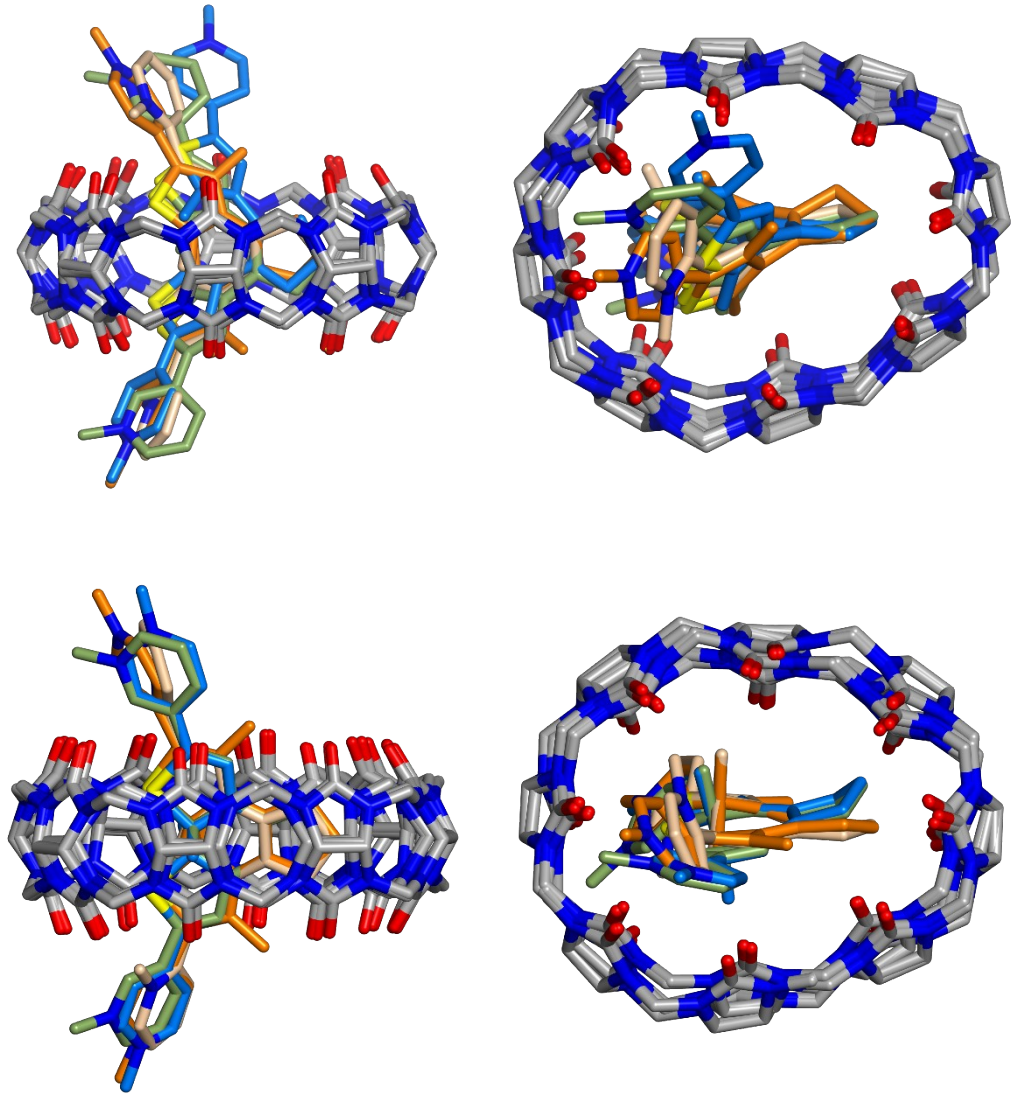

Figure S19 – (Top) superimposition of guests **1o** (orange), **2o** (blue), **3o** (green), and **4o** (wheat) inside the CB8 host; (bottom) superimposition of guests **1c** (orange), **2c** (blue), **3c** (grey), and **4c** (wheat) inside the CB8 host. The structures were optimized at the ωB97X-D/6-31G* level employing the SMD model for solvation in water starting from the fully inserted lowest-energy conformer generated by CREST.

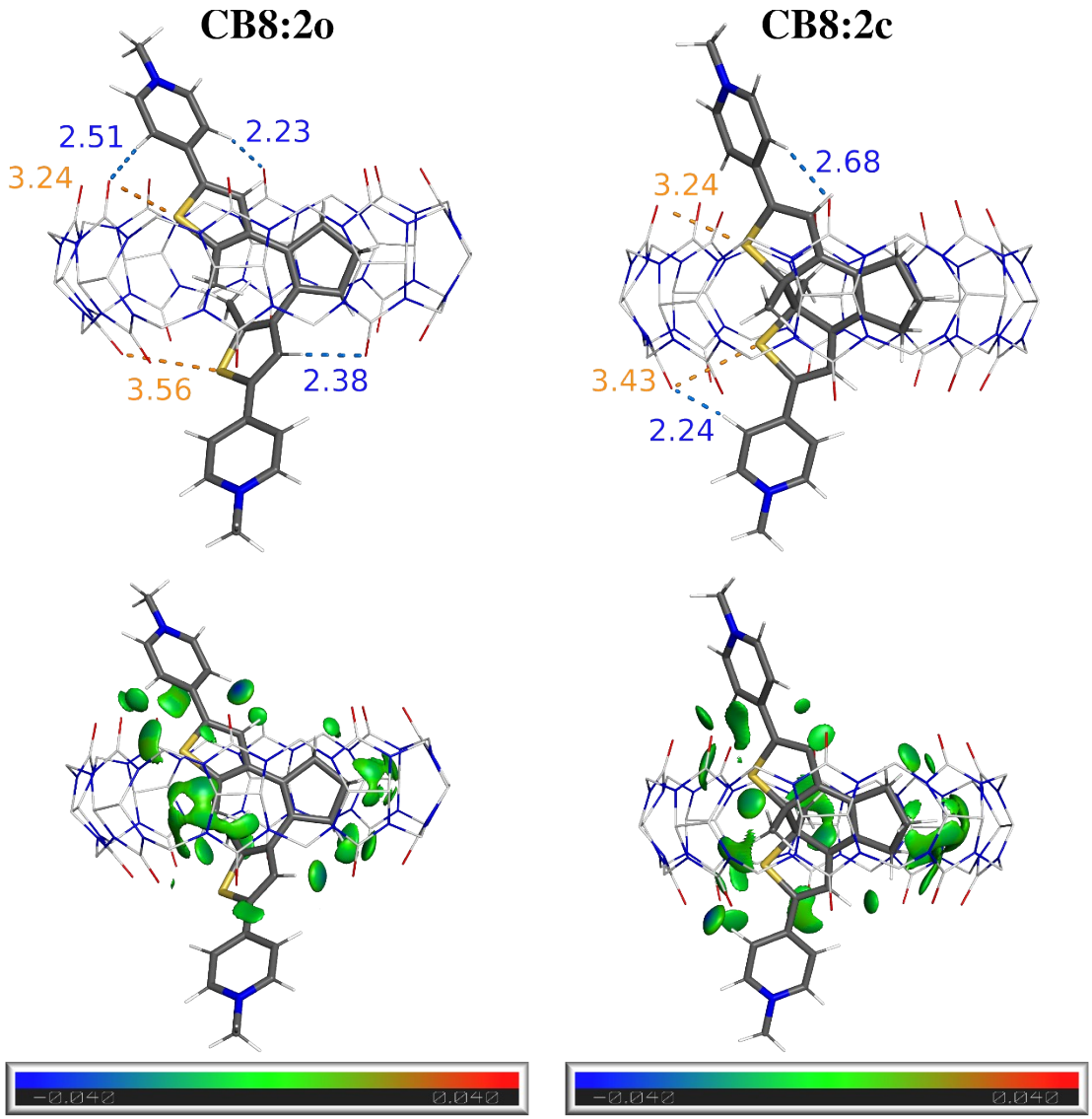

Figure S20 – Top: DFT-optimized structure (ωB97X-D/6-31G*; water) of CB8:**2o** and CB8:**2c** with the distances (Å) of the most relevant interactions shown in orange (S···O) or blue (C-H···O). Bottom: IGM analysis using a δg^{inter} isosurface of 0.008 a.u. and a BGR color code in the range −0.040 < ρ sign (λ_2) < 0.040 a.u.

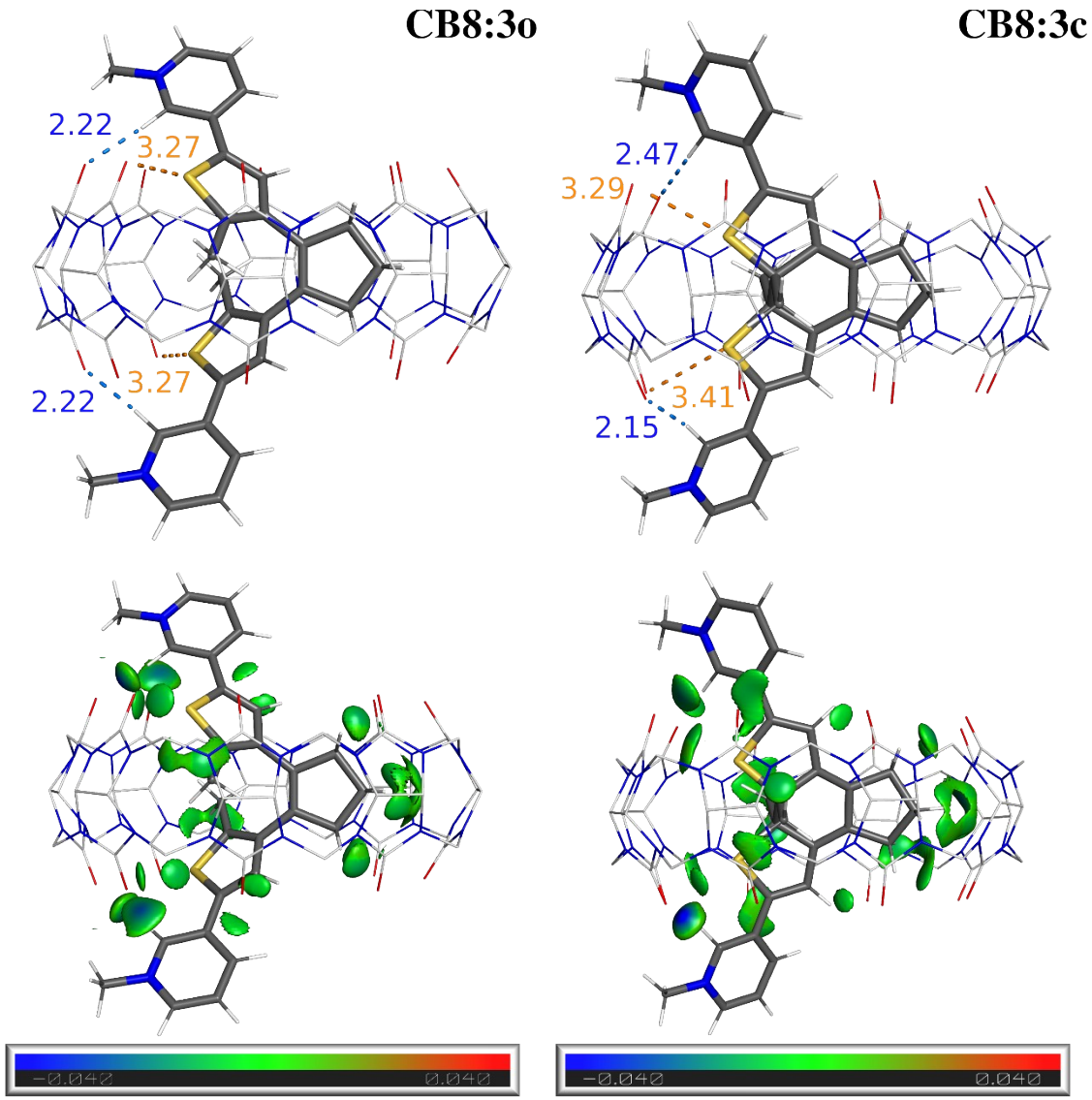

Figure S21 – Top: DFT-optimized structure (ωB97X-D/6-31G*; water) of CB8:**3o** and CB8:**3c** with the distances (Å) of the most relevant interactions shown in orange (S···O) or blue (C-H···O). Bottom: IGM analysis using a δg^{inter} isosurface of 0.008 a.u. and a BGR color code in the range $-0.040 < \rho$ sign $(\lambda_2) < 0.040$ a.u.

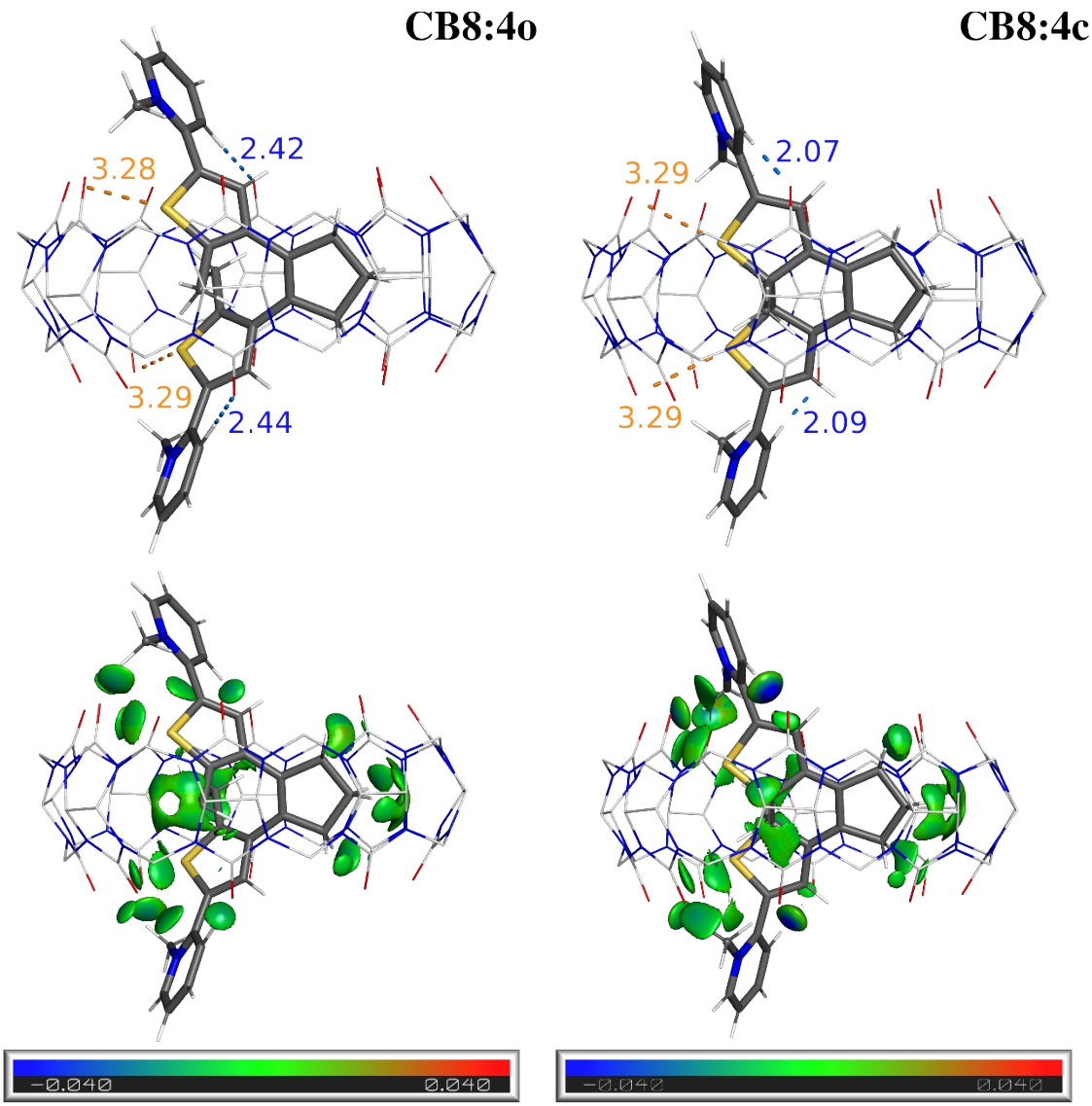

Figure S22 – Top: DFT-optimized structure (ωB97X-D/6-31G*; water) of CB8:**4o** and CB8:**4c** with the distances (Å) of the most relevant interactions shown in orange (S···O) or blue (C-H···O). Bottom: IGM analysis using a δg^{inter} isosurface of 0.008 a.u. and a BGR color code in the range $-0.040 < \rho$ sign $(\lambda_2) < 0.040$ a.u.

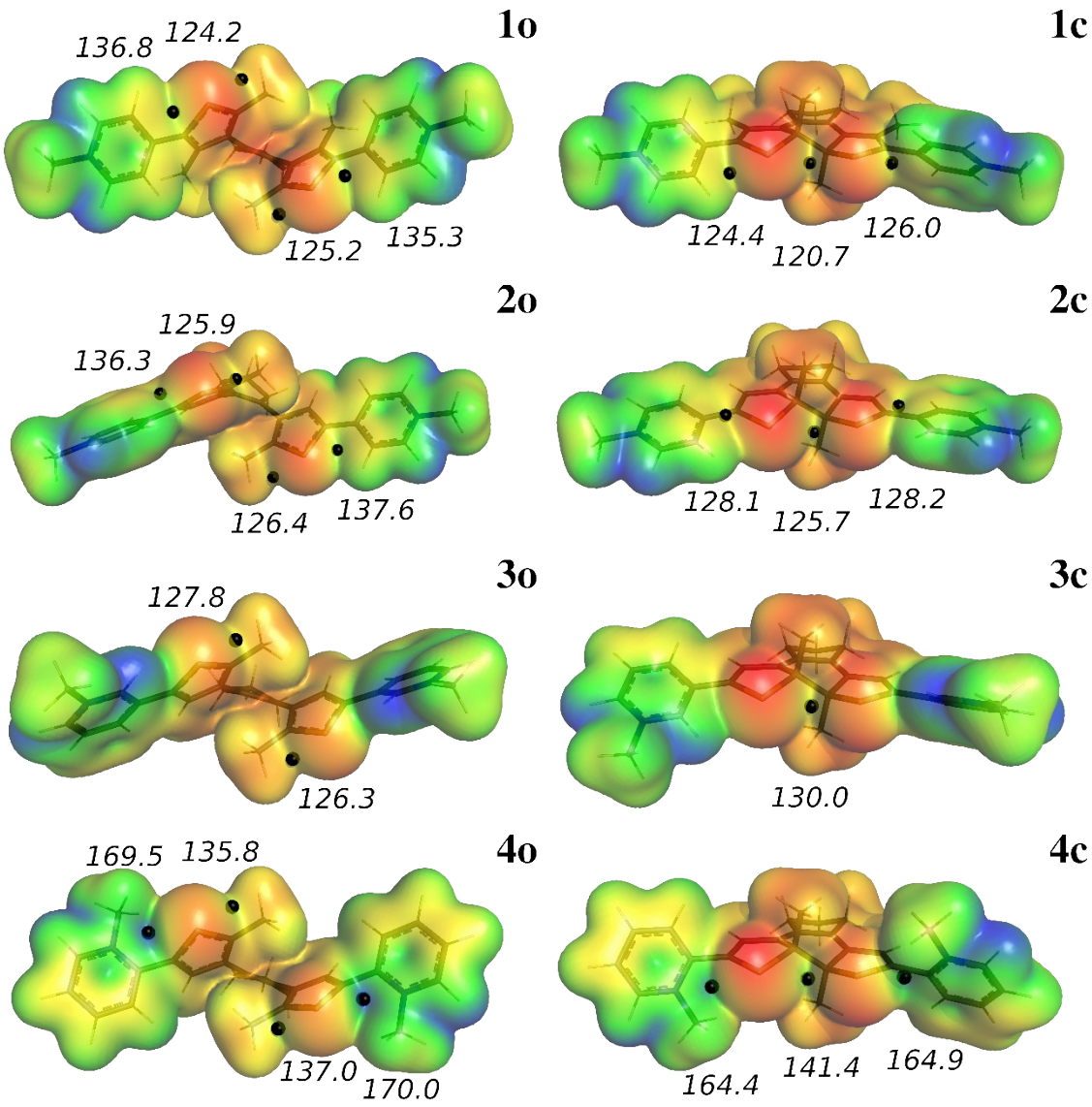

Figure S23 – Electrostatic potential of DTEs **1o-4a** (left) and **1c-4c** (right) mapped on the 0.004 au contour of the electron density. The maxima associated with the sulfur atoms, V_{max}, corresponding to the σ-holes are shown as black dots along with the values (in kcal mol^{-1}). For the specific case of **3o** and **3c**, the maximum located on the side of the pyridinium substituent could not be unequivocally discriminated from the one arising from the N-Me^{+}.

Table S1 – Collected S···O distances (Å) and C−S···O distances (degrees) for all the studied systems. In bold are highlighted the values fulfilling the classical chalcogen bonding criterion (less than the sum of vdW radii, S···O distances < 3.39 Å[19] and C−S···O angles of 150–180°.[20] The V_{max} values corresponding to the σ-holes for each guest are also shown.

	S···O distance / Å	C−S···O angles / °	V_{max} / kcal mol^{-1}
CB8:**1o**	**3.19**	134	136.8, 124.2, 125.2, 135.3
	3.19	137	
CB8:**1c**	3.41	165	126.0, 125.4, 120.7
	3.39	**164**	
CB8:**2o**	**3.24**	134	136.3, 125.9, 126.4, 137.6
	3.56	138	
CB8:**2c**	**3.24**	**155**	128.1, 125.7, 128.2
	3.43	145	
CB8:**3o**	**3.27**	147	127.8, 126.3
	3.27	147	
CB8:**3c**	**3.29**	**161**	130.0
	3.41	145	
CB8:**4o**	**3.29**	**151**	169.5, 135.8, 137.0, 170.5
	3.28	**151**	
CB8:**4c**	**3.29**	**160**	165.4, 141.4, 165.9
	3.29	**160**	

6. NMR data

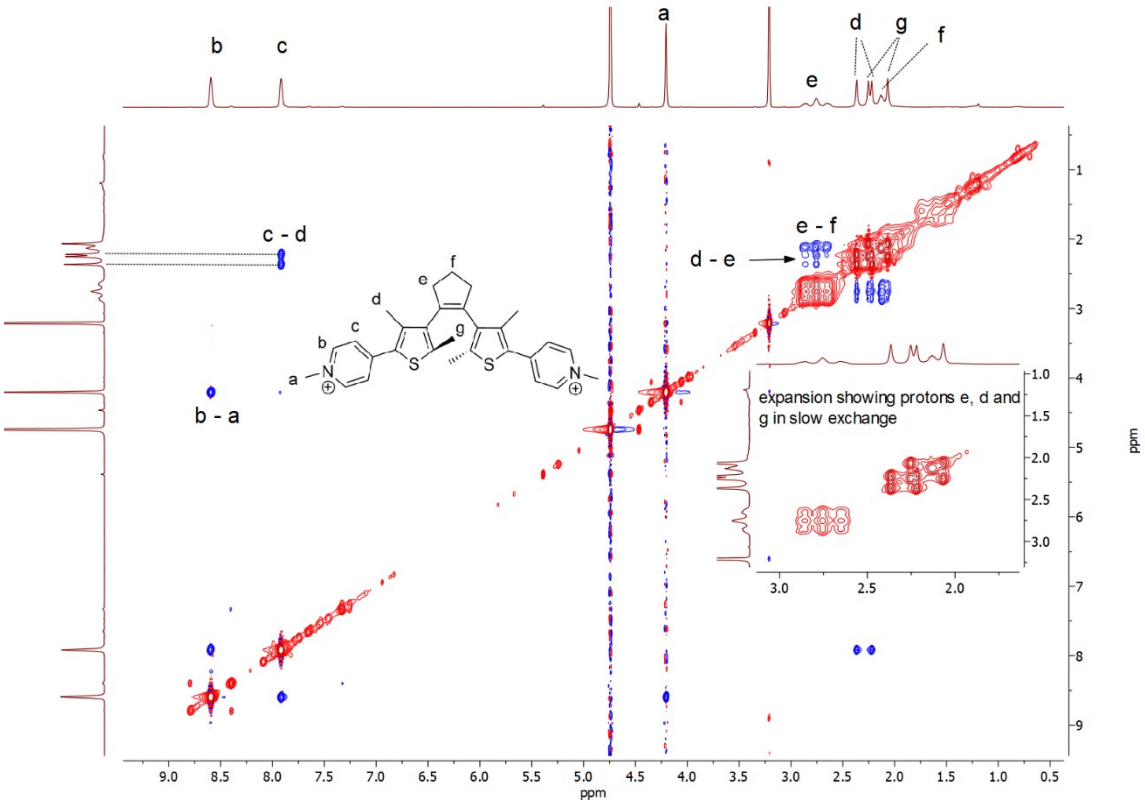

Figure S24 –NOESY (400 MHz) of DTE **1o** in CD_3OD at 25 °C.

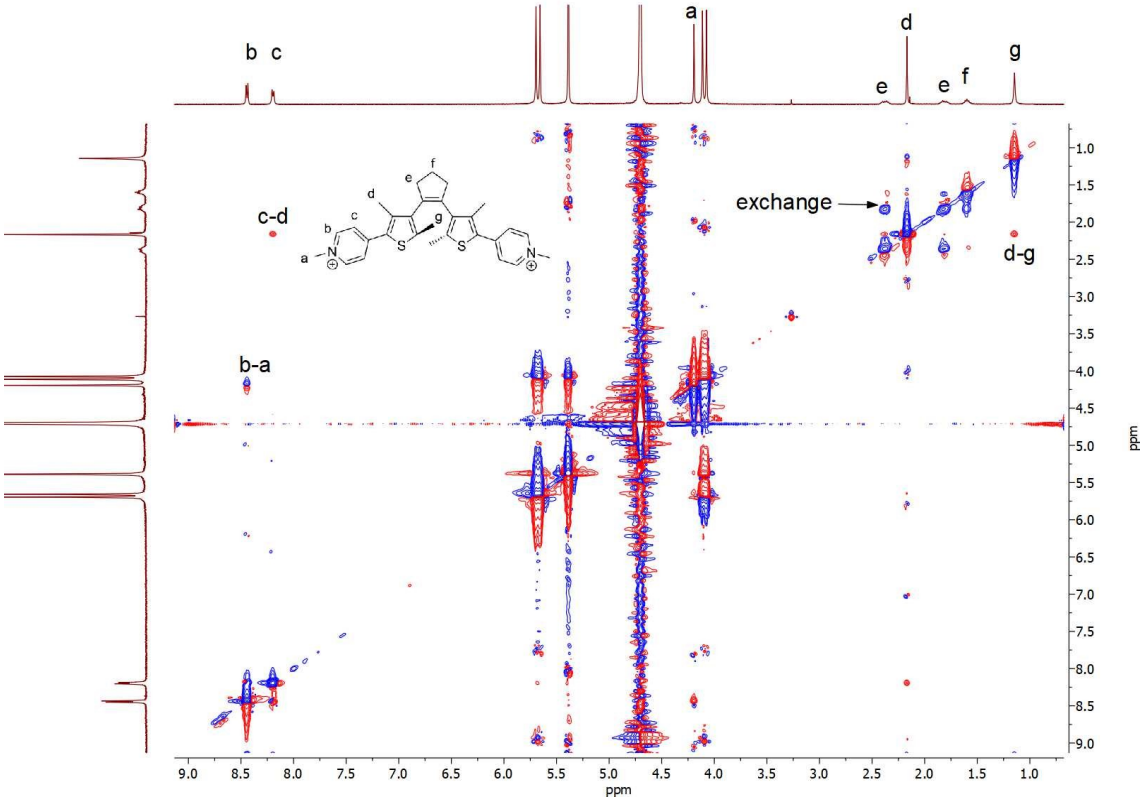

Figure S25 –ROESY (400 MHz) of DTE **1o** with 1 equiv. of CB8 in D_2O at 25 °C.

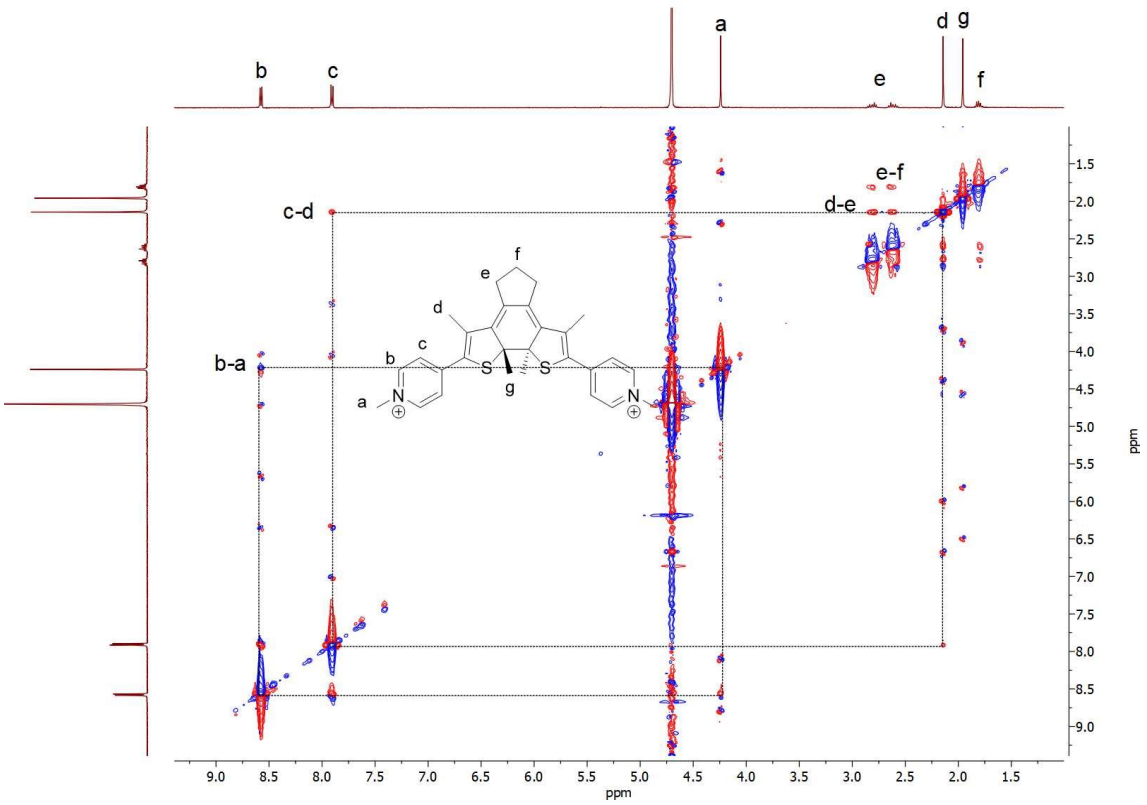

Figure S26 –ROESY (400 MHz) of DTE **1c** in D_2O at 25 °C.

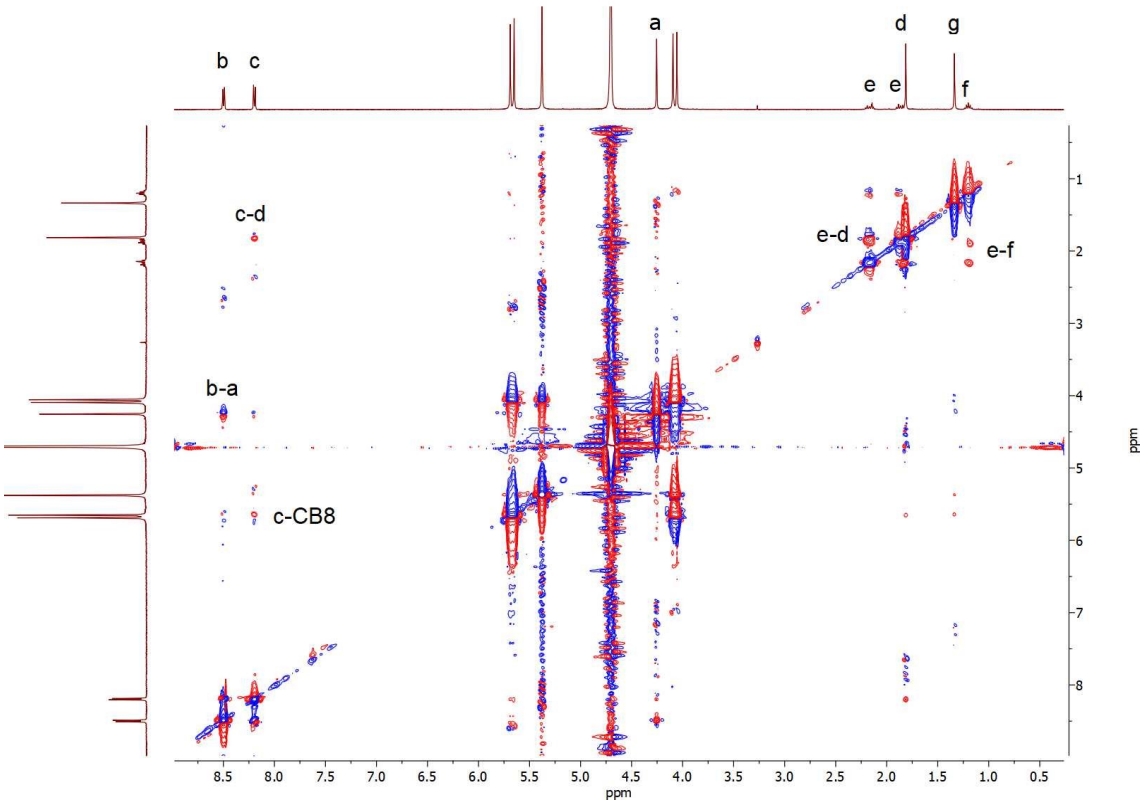

Figure S27 –ROESY (400 MHz) of DTE **1c** with 1 equiv. of CB8 in D_2O at 25 °C.

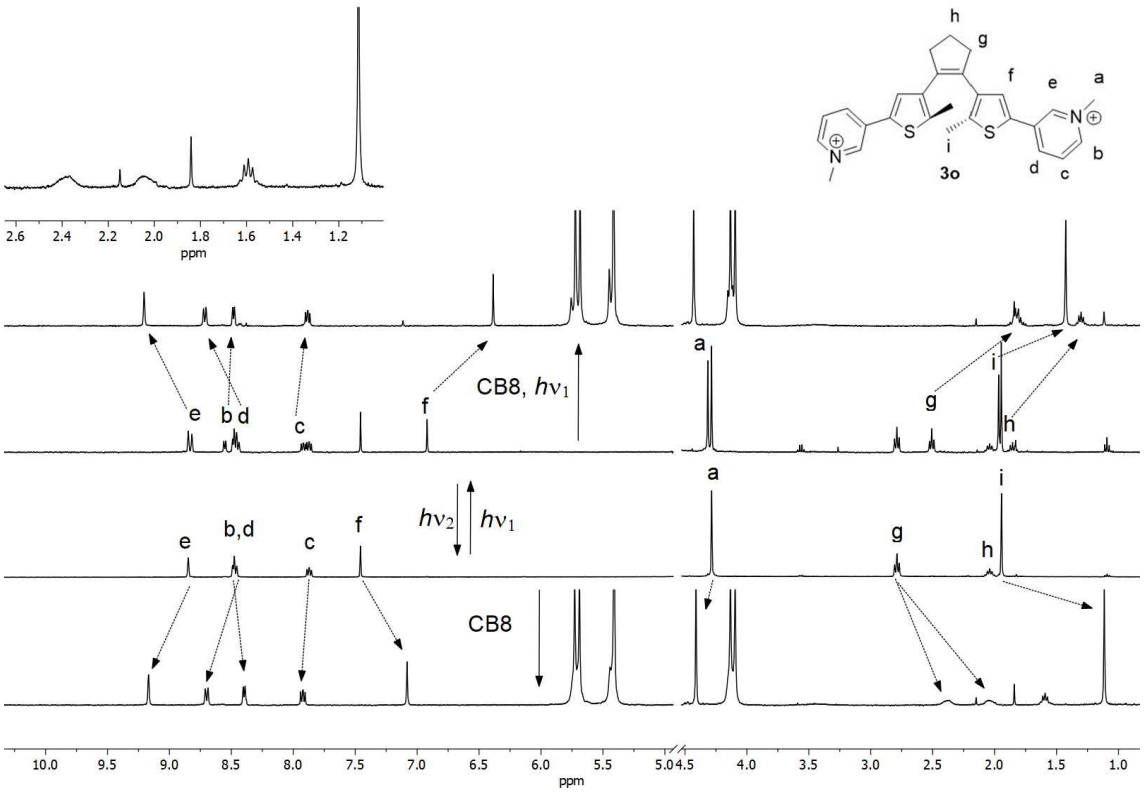

Figure S28 – ^{1}H NMR (400 MHz) spectra of **3o**/**3c** (0.5 mM in D_2O) in the absence and in the presence of 1.2 equiv. of CB8. $h\nu_1$ > 500 nm and $h\nu_2$ = 365 nm.

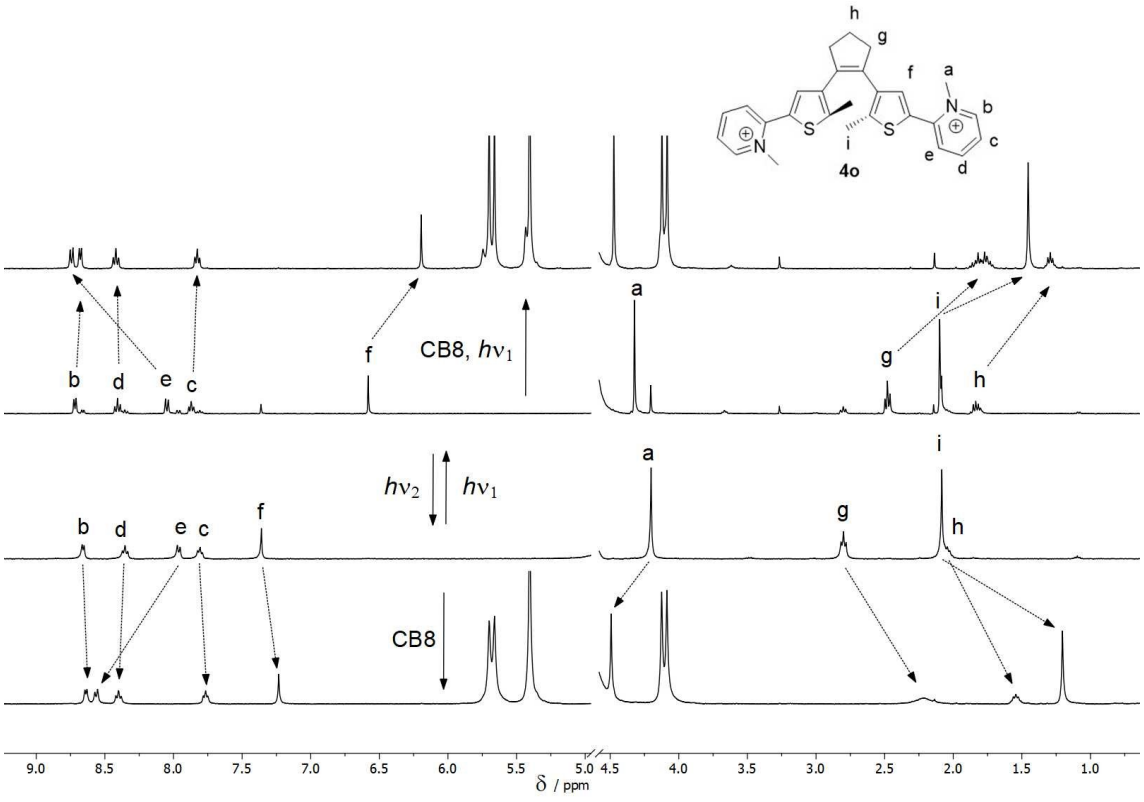

Figure S29 – ^{1}H NMR (400 MHz) spectra of **4o**/**4c** (0.5 mm in D_2O) in the absence and in the presence of 1.2 equiv. of CB8. $h\nu_1$ > 500 nm and $h\nu_2$ = 365 nm.

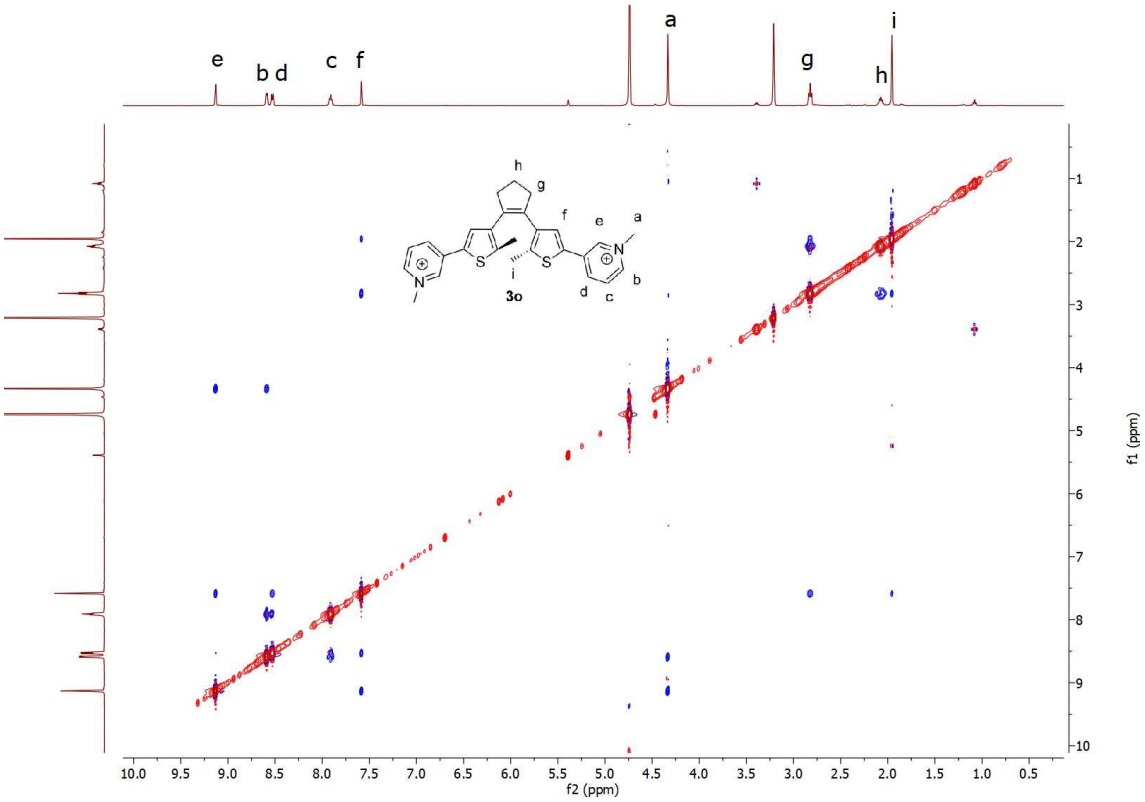

Figure S30 – NOESY (400 MHz) of DTE **3o** in CD_3OD.

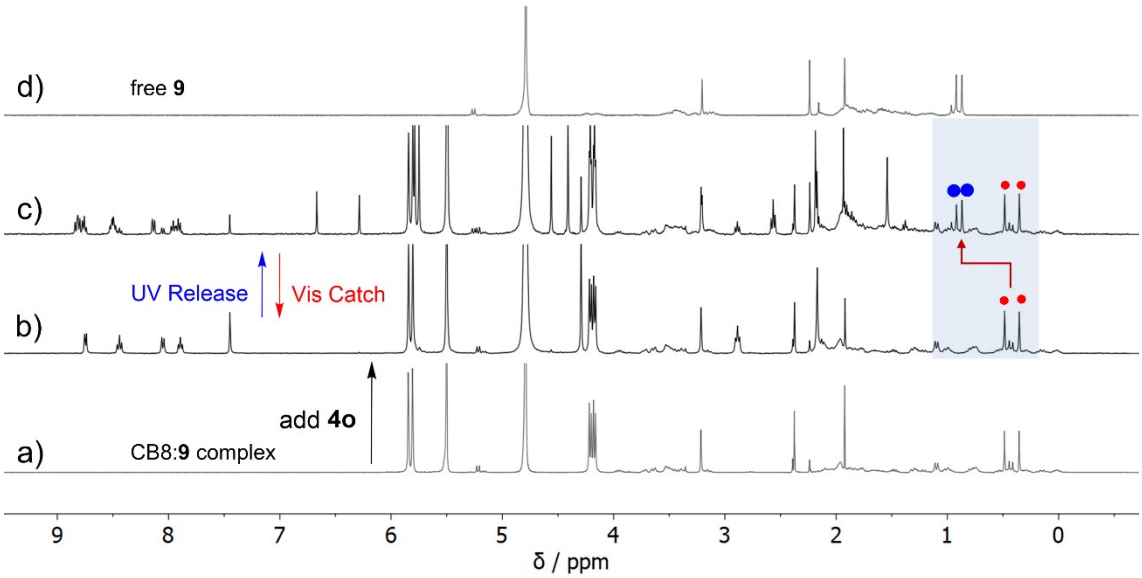

Figure S31 – ^{1}H NMR experiments demonstrating the light-controlled binding and release of vecuronium **9** using DTE **4** as a competitor with photocontrolled affinity. 400 MHz ^{1}H NMR spectra of (a) CB8:**9** host:guest complex (1 mM);(b) a solution containing CB8 (1 mM), **9** (1 mM) and DTE **4o** (1.2 mM); (c) the same as in (b) upon irradiation with 365 nm until reaching the PSS (d) ^{1}H NMR spectrum of **9** (1 mM). All solutions were prepared in the D_2O and the spectra acquired at 25 ºC.

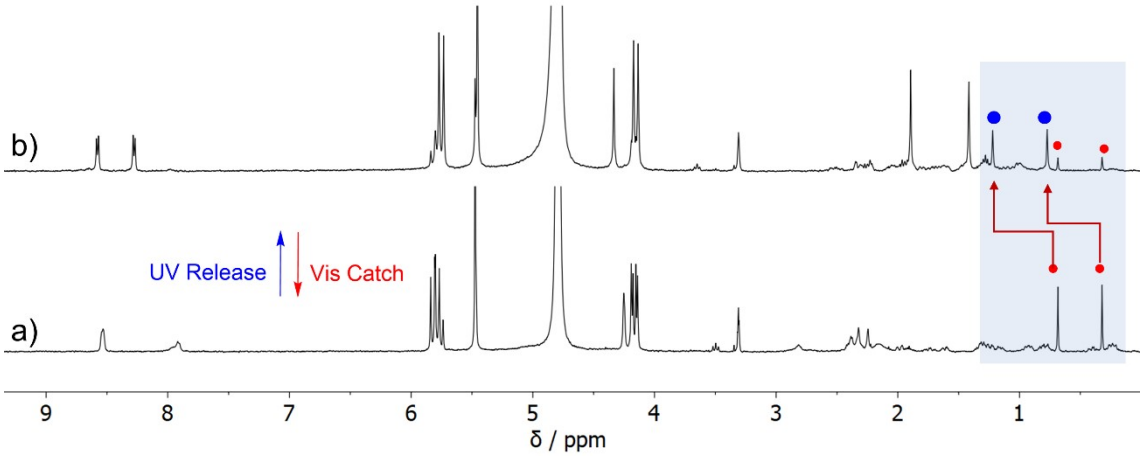

Figure S32 – ^{1}H NMR experiments demonstrating the light-controlled binding and release of testosterone **8** using DTE **1** as a competitor with photocontrolled affinity. 400 MHz ^{1}H NMR spectra of (a) a solution containing CB8 (0.2 mM), **8** (0.2 mM) and DTE **1o** (0.2 mM); (b) the same as in (a) upon irradiation with 365 nm until reaching the PSS. All solutions were prepared in the D_2O:CD_3OD (98:2) and the spectra acquired at 25 ºC. CD_3OD was used to help the solubilization of testosterone.

7. Photochemical Characterization

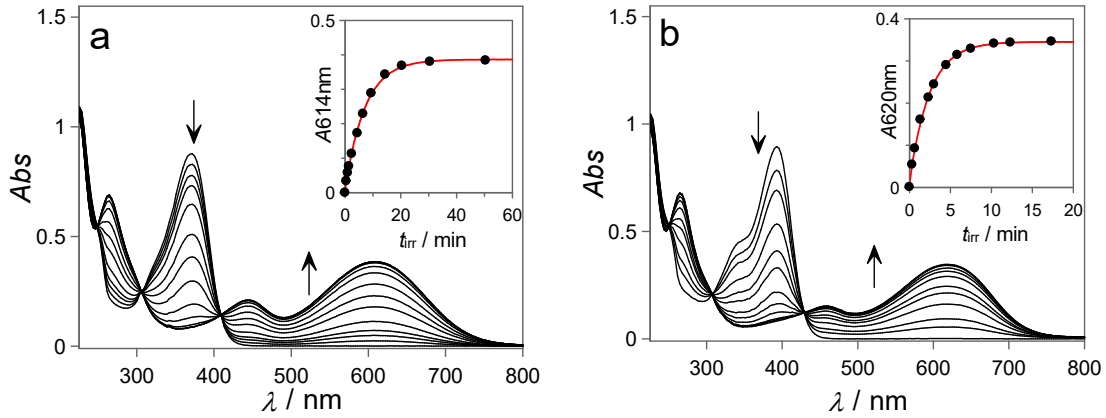

Figure S33 – (a) Spectral variations observed upon irradiation of **1o** (22 μM in H_2O) with 365 nm UV light; $\phi_{o\text{-}c}$ = 0.04. (b) The same for **1o** (22 μM in H_2O) in the presence of 1 equivalent of CB8; $\phi_{o\text{-}c}$ = 0.14.

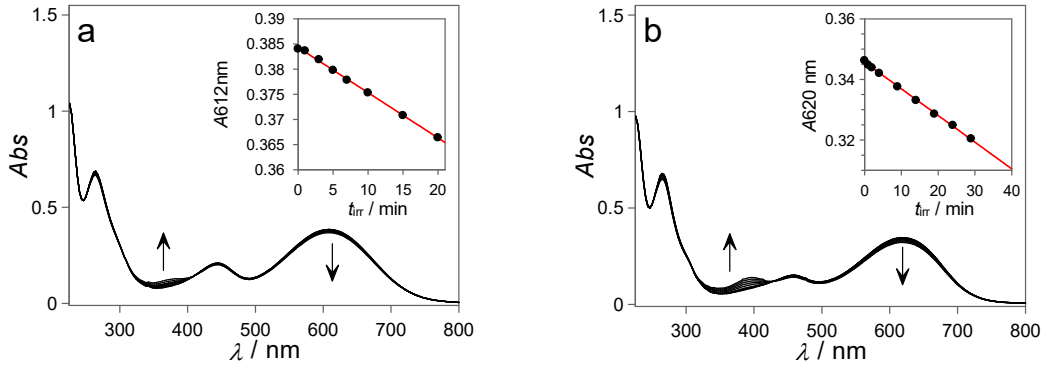

Figure S34 – (a) Spectral variations observed upon irradiation of **1c** (22 μM in H_2O) with 550 nm light; ϕ = 0.001. (b) The same for **1c** (22 μM in H_2O) in the presence of 1 equivalent of CB8; ϕ = 0.001.

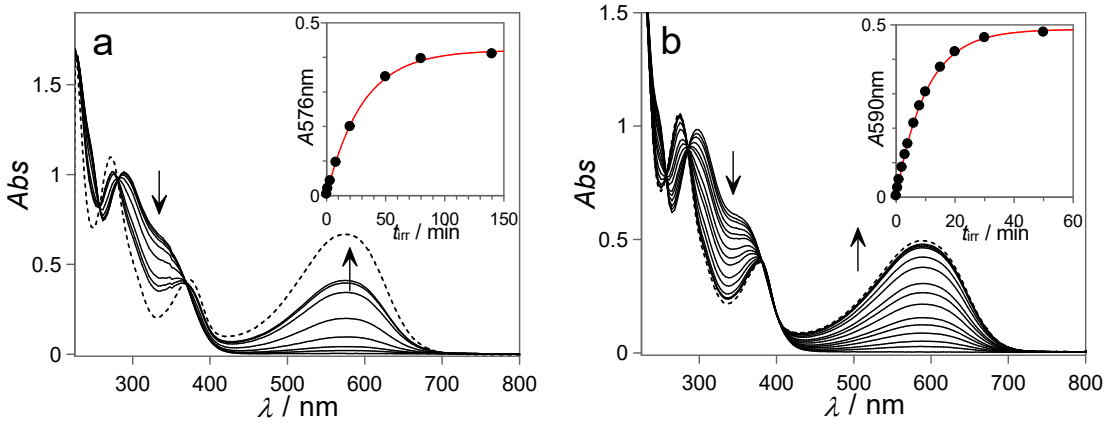

Figure S35– (a) Spectral variations observed upon irradiation of **3o** (48 μM in H_2O) with 334 nm UV light; ϕ = 0.003; the fraction of **3c** at the PSS was estimated to be 61%. (b) The same for **3o** (52 μM in H_2O) in the presence of 1 equivalent of CB8; ϕ = 0.011; the fraction of **3c:CB8** at the PSS was estimated to be 95%. The dotted line spectra correspond to pure **3c**/**3c:CB8**, obtained upon spectral decomposition.

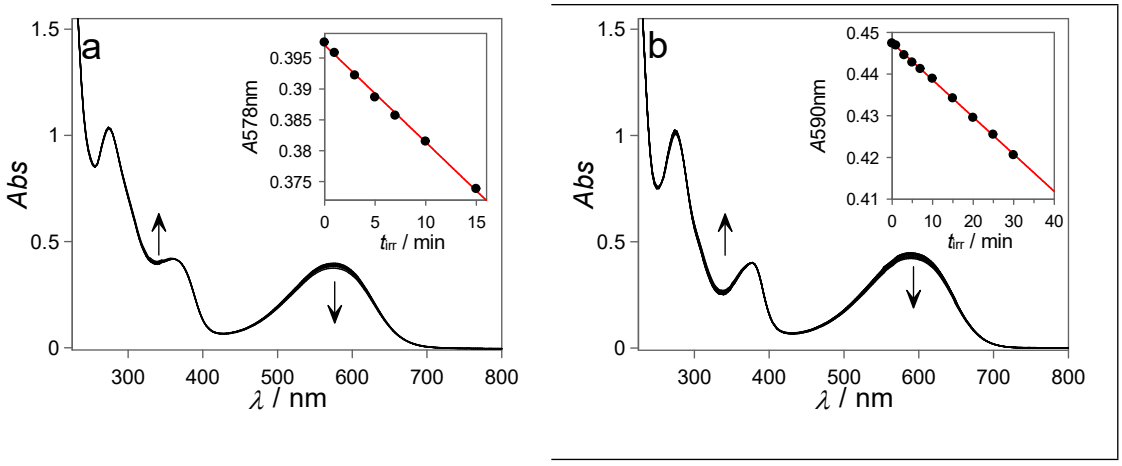

Figure S36 – (a) Spectral variations observed upon irradiation of **3c** (48 μM in H_2O) with 550 nm light; ϕ = 0.0014; (b) The same for **3c** (48 μM in H_2O) in the presence of 1 equivalent of CB8; ϕ = 0.0010.

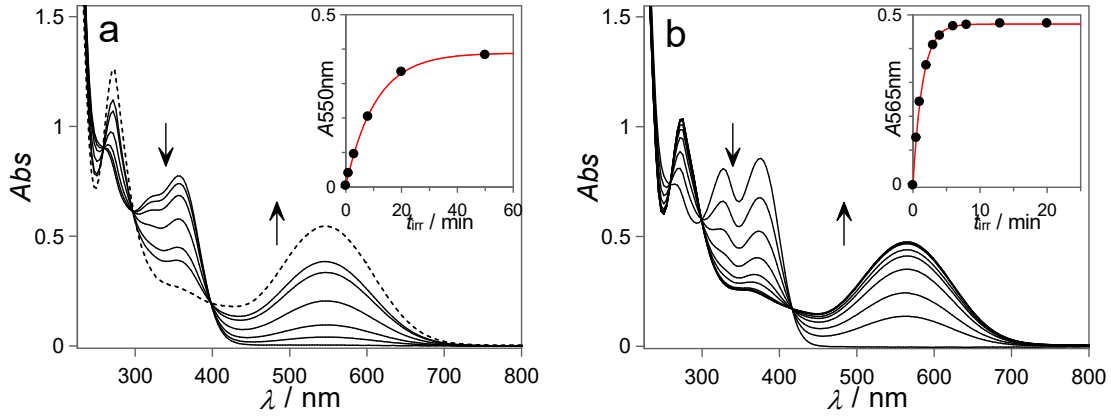

Figure S37 – (a) Spectral variations observed upon irradiation of **4o** (60 μM in H_2O) with 334 nm UV light; ϕ = 0.009; the fraction of **4c** at the PSS was estimated to be 70%. (b) The same for **4o** (60 μM in H_2O) in the presence of 1 equivalent of CB8; ϕ = 0.087; the fraction of **4c:CB8** at the PSS was estimated to be 100%. The dotted line spectra correspond to pure **4c**/**4c:CB8**, obtained upon spectral decomposition.

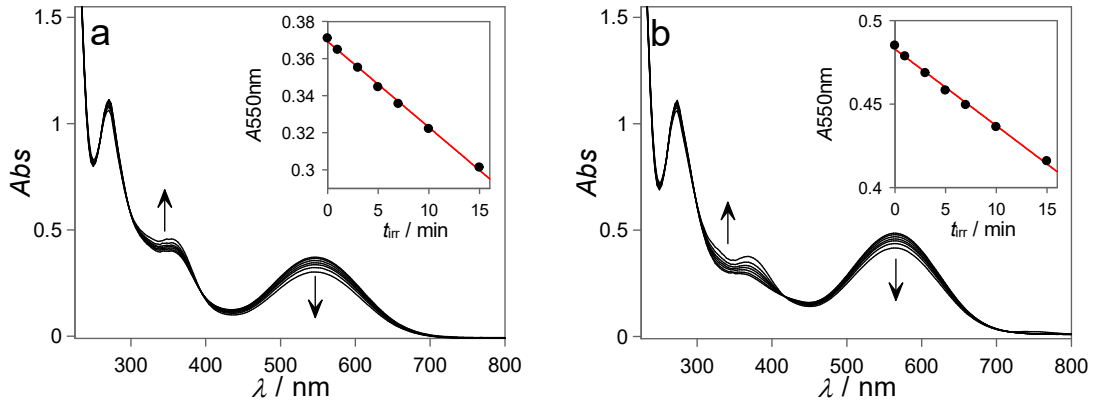

Figure S38 –(a) Spectral variations observed upon irradiation of **4c** (60 μM in H_2O) with 550 nm light; ϕ = 0.0058. (b) The same for **4c** (60 μM in H_2O) in the presence of 1 equivalent of CB8; ϕ = 0.0054.

8. References

1 A. Day, A. P. Arnold, R. J. Blanch and B. Snushall, Controlling factors in the synthesis of cucurbituril and its homologues., *J. Org. Chem.*, 2001, **66**, 8094–8100.

2 S. Yi and A. E. Kaifer, Determination of the Purity of Cucurbit[n]uril (n = 7, 8) Host Samples, *J. Org. Chem.*, 2011, **76**, 10275–10278.

3 C. G. Hatchard and C. A. Parker, A New Sensitive Chemical Actinometer. II. Potassium Ferrioxalate as a Standard Chemical Actinometer, *Proc. R. Soc. A Math. Phys. Eng. Sci.*, 1956, **235**, 518–536.

4 R. Göstl, B. Kobin, L. Grubert, M. Pätzel and S. Hecht, Sterically Crowding the Bridge of Dithienylcyclopentenes for Enhanced Photoswitching Performance, *Chem. - A Eur. J.*, 2012, **18**, 14282–14285.

5 X. Yao, T. Li, S. Wang, X. Ma and H. Tian, A photochromic supramolecular polymer based on bis-p-sulfonatocalix[4]arene recognition in aqueous solution, *Chem. Commun.*, 2014, **50**, 7166.

6 C. Yu, B. Hu, C. Liu and J. Li, Design, syntheses and photochromic properties of dithienylcyclopentene optical molecular switches, *J. Phys. Org. Chem.*, 2017, **30**, e3584.

7 W. Tan, Q. Zhang, J. Zhang and H. Tian, Near-Infrared Photochromic Diarylethene Iridium (III) Complex, *Org. Lett.*, 2009, **11**, 161–164.

8 P. Pracht, F. Bohle and S. Grimme, Automated exploration of the low-energy chemical space with fast quantum chemical methods, *Phys. Chem. Chem. Phys.*, 2020, **22**, 7169–7192.

9 S. Grimme, Exploration of Chemical Compound, Conformer, and Reaction Space with Meta-Dynamics Simulations Based on Tight-Binding Quantum Chemical Calculations, *J. Chem. Theory Comput.*, 2019, **15**, 2847–2862.

10 C. Bannwarth, S. Ehlert and S. Grimme, GFN2-xTB—An Accurate and Broadly Parametrized Self-Consistent Tight-Binding Quantum Chemical Method with Multipole Electrostatics and Density-Dependent Dispersion Contributions, *J. Chem. Theory Comput.*, 2019, **15**, 1652–1671.

11 S. Grimme, Semi-Empirical Extended Tight-Binding Program Package Xtb.v-6.4.0. Mulliken Center for Theoretical Chemistry, University of Bonn: Bonn, Germany 2020.

12 J.-D. Chai and M. Head-Gordon, Long-range corrected hybrid density functionals with damped atom–atom dispersion corrections, *Phys. Chem. Chem. Phys.*, 2008, **10**, 6615.

13 M. J. Frisch, G. W. Trucks, H. B. Schlegel, G. E. Scuseria, M. A. Robb, J. R. Cheeseman, G. Scalmani, V. Barone, G. A. Petersson, H. Nakatsuji, M. C. X. Li, A. Marenich, J. Bloino, B. G. Janesko, R. Gomperts, B. Mennucci, H. P. Hratchian, J. V. Ortiz, A. F. Izmaylov, J. L. Sonnenberg, D. Williams-Young, F. Ding, F. Lipparini, F. Egidi, J. Goings, B. Peng, A. Petrone, T. Henderson, D. Ranasinghe, V. G. Zakrzewski, J. Gao, N. Rega, G. Zheng, W. Liang, M. Hada, M. Ehara, K. Toyota, R. Fukuda, J. Hasegawa, M. Ishida, T. Nakajima, Y. Honda, O. Kitao, H. Nakai, T. Vreven, K. Throssell, J. A. Montgomery Jr., J. E. Peralta, F. Ogliaro, M. Bearpark, J. J. Heyd, E. Brothers, K. N. Kudin, V. N. Staroverov, T. Keith, R. Kobayashi, J. Normand, K. Raghavachari, A. Rendell, J. C. Burant, S. S. Iyengar, J. Tomasi, M. Cossi, J. M. Millam, M. Klene, C. Adamo, R. Cammi, J. W. Ochterski, R. L. Martin, K. Morokuma, O. Farkas, J. B. Foresman and D. J. Fox, Gaussian 09. Gaussian Inc.: Wallingford, CT 2009.

14 A. V. Marenich, C. J. Cramer and D. G. Truhlar, Universal Solvation Model Based on Solute Electron Density and on a Continuum Model of the Solvent Defined by the Bulk Dielectric Constant and Atomic Surface Tensions, *J. Phys. Chem. B*, 2009, **113**, 6378–6396.

15 T. Lu and F. Chen, Multiwfn: A multifunctional wavefunction analyzer, *J. Comput. Chem.*, 2012, **33**, 580–592.

16 http://igmplot.univ-reims.fr/index.php.

17 C. Lefebvre, H. Khartabil, J.-C. Boisson, J. Contreras-García, J.-P. Piquemal and E. Hénon, The Independent Gradient Model: A New Approach for Probing Strong and Weak Interactions in Molecules from Wave Function Calculations, *ChemPhysChem*, 2018, **19**, 724–735.

18 C. Lefebvre, G. Rubez, H. Khartabil, J.-C. Boisson, J. Contreras-García and E. Hénon, Accurately extracting the signature of intermolecular interactions present in the NCI plot of the reduced density gradient versus electron density, *Phys. Chem. Chem. Phys.*, 2017, **19**, 17928–17936.

19 M. Mantina, A. C. Chamberlin, R. Valero, C. J. Cramer and D. G. Truhlar, Consistent van der Waals Radii for the Whole Main Group, *J. Phys. Chem. A*, 2009, **113**, 5806–5812.

20 K. Kříž, J. Fanfrlík and M. Lepšík, Chalcogen Bonding in Protein−Ligand Complexes: PDB Survey and Quantum Mechanical Calculations, *ChemPhysChem*, 2018, **19**, 2540–2548.